

**Atomic Dynamics and
Anomalous Thermodynamic
Behavior of Novel Compounds**

**Phase distribution
study for U-Zr-metallic
simfuel**



Bi-monthly • May - June • 2016

ISSN: 0976-2108

BARC

NEWSLETTER



SHIP BORNE TERMINAL

CONTENTS

Editorial Committee

Chairman

Dr. G.K. Dey
Materials Group

Editor

Dr. G. Ravi Kumar
SIRD

Members

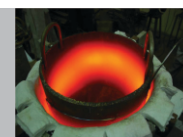
Dr. G. Rami Reddy, RSD
Dr. A.K. Tyagi, Chemistry Divn.
Dr. S. Kannan, FCD
Dr. C.P. Kaushik, WMD
Dr. S. Mukhopadhyay,
Seismology Divn.
Dr. S.M. Yusuf, SSPD
Dr. B.K. Sapra, RP&AD
Dr. J.B. Singh, MMD
Dr. S.K. Sandur, RB&HSD
Dr. R. Mittal, SSPD
Dr. Smt. S. Mukhopadhyay, ChED



BARC develops Control Systems of
Ship Borne Terminal for
The Indian Space programme

1

Development of 50kW, 2-3kHz Induction
Heating Inverter for WIP, Trombay



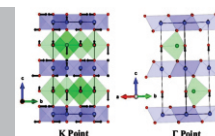
2



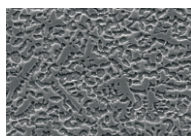
Development & Deployment of
BARC Vessel Inspection System
(BARVIS) for TAPS-1&2

3

Atomic Dynamics and Anomalous
Thermodynamic Behavior of
Novel Compounds



12



Phase distribution study for
U-Zr-metallic simfuel

17

Indigenous technology development:
Seismic Switch for Nuclear Reactors



24



TAFICS Theme Meeting on I&C Security
Program For Nuclear Facilities

28

Thirty First Training Course on Basic
Radiological Safety and Regulatory
Measures for Nuclear Facilities”



30



Technology Transfer to Industries

31

60th DAE Solid State Physics
Symposium-2015 (Diamond Jubilee Year)



36



National Technology Day 2016

37

BARC Training School Graduation
of the 59th batch of OCES and
12th batch of OCDF trainees



39



Scientists Honoured

41

BARC develops Control Systems of Ship Borne Terminal for The Indian Space programme

RCnD, BARC has recently completed the design and fabrication of the Servo controller and 3 axis drives for the 4.6 m Ship-borne terminal to be deployed in support of ISRO's launch and recovery missions. This would now be subjected to further integration, trials and qualification tests at ECIL.

ISRO Telemetry Tracking and Command Network provides TTC (Telemetry, Tracking and Control) support for Launch Vehicles and Spacecrafts for all ISRO missions. BARC and ECIL are developing this

remote high seas where future manned reentry and recovery capsules might land. Also TTC terminals located at strategic high sea locations are critical so as to provide an uninterrupted coverage and backup during launches.

This indigenous development is being carried-out by BARC and ECIL in the framework of a contract by ISTRAC/ISRO on ECIL.

The unit is undergoing integration, functional and qualification tests on an indigenously developed single axis ship motion simulator. ISRO is expected to deploy several more SBTs in future.

RCnD, BARC is responsible for the development of the three axis gimbals, controller electronics and the motor drives. BARC has also designed the drive unit for the rapid deployment tilting mechanism and interlocks for the SBT. Earlier, BARC in association with ECIL had successfully developed a variety of antenna pedestals and controllers of various sizes for ground station applications for tracking satellites and RPVs. India's first deep space network terminal – the 32 metre antenna- which was deployed for the Indian moon and mars missions was developed by ECIL in collaboration with BARC.

Fig. 2: Three axis pedestal without reflector



Fig. 1: Antenna Control and Drive Unit Cabinet



indigenous ship borne antenna terminal (SBT) to support ISRO missions which include tracking of re-entry vehicles for future Indian manned missions to space. This 4.6m ship-borne terminal is capable of continuously pointing at the commanded angles and mono-pulse tracking even in the presence of ship's rocking movements. The antenna is actively stabilized against ship movements by the use of an Inertial Measurement Unit. The SBT is mounted on a rugged chassis which is designed to be easily transported in standard ISO shipping containers. The reflector of the SBT can be quickly disassembled and the SBT can be folded down automatically for swift relocation and redeployment. The SBT technology is crucial as it extends the TTC capability to be provided even in the

Development of 50kW, 2-3kHz Induction Heating Inverter for WIP, Trombay

R.K. Sadhu, B. Maurya and B.M. Barapatre
ATSS, E&I Group

Induction Heating Inverters are required for five-zone induction furnace of Waste Immobilization Plant (WIP), Trombay; used for nuclear waste immobilization through vitrification process under Indian Nuclear Waste Management Programme. The electrical power to each zone is supplied by individual 50kW, 2-3kHz Induction Heating Inverter. This inverter has been designed by Advanced Technology Systems Section (ATSS), E&I Group, BARC and mass-produced at ECIL, Hyderabad. Involving ECIL in mass-production of these inverters would serve long-term strategic requirements of Indian Nuclear Waste Management Programme including maintenance for their operating-life.

After satisfactory Factory Acceptance Tests (FAT) at ECIL, ten units of these inverters have been delivered to WIP, Trombay.

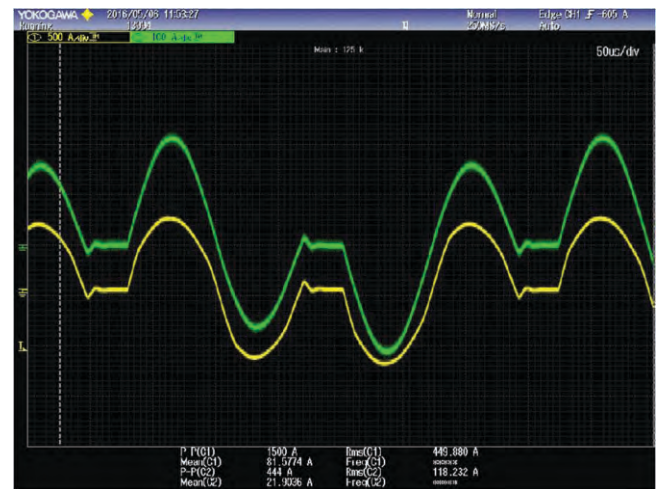


Induction Furnace Heating (~925°C)

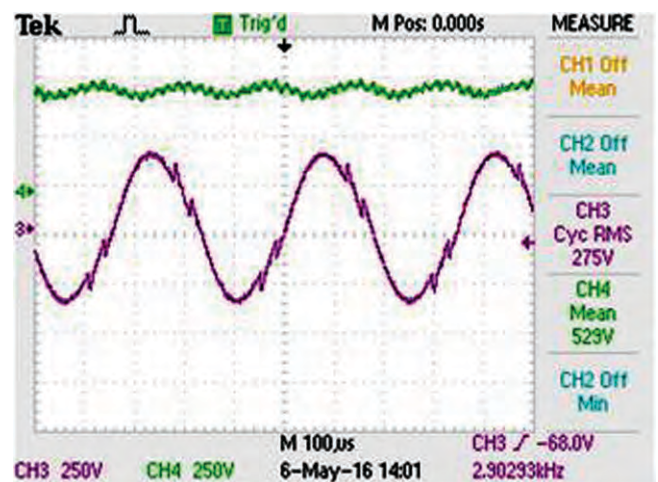


50kW Induction Heating Inverter

SCR based half-bridge inverter configuration having 3-phase diode rectifier at its front end and current transformer at rear end is used in these inverters for DC to AC conversion; resulting most reliable system. These are designed with state-of-art technology and with all relevant control & protections required for such power electronics systems. All major heat-generating components (e.g. diode-bridge, DC filter capacitor, commutation capacitor & choke, inverter SCR & diode, current transformer etc.) of these inverters are water-cooled; resulting very compact packaging.



Primary (yellow) & Load (green) Current



Load (pink) & DC-bus (green) Voltage

Development & Deployment of BARC Vessel Inspection System (BARVIS) for TAPS-1&2

Jit Pal Singh, R. Ranjon, M.P. Kulkarni and N.L. Soni

Refuelling Technology Division

R.J. Patel

Reactor Design & Development Group

As per regulatory requirements, inspection of welds in Reactor Pressure Vessel (RPV) is necessary for further continuing operation of TAPS-1&2. Upper shell longitudinal welds of RPV which were seen as inaccessible up till now have been inspected first time since operation of the reactors by deploying Weld Inspection Manipulator (WIM) in Unit #1 in August 2012. Subsequently Unit #2 and again Unit#1 upper shell welds were inspected with upgraded versions of WIM in Feb 2013 & March 2015 respectively. Inspection of upper shell welds paves the way for more challenging inspection of beltline region welds. These welds are accessible only from Inside Diameter (ID) surface through a narrow annular gap of 25 mm between RPV wall and thermal shield by managing obstructions due to core internals. **BARC Vessel Inspection System (BARVIS)** for inspection of beltline region welds from inner side of the RPV was designed, manufactured, tested and qualified for sending scanning probes in to the annular gap of 25mm as per RPV engineering drawings and also based on actual gap measured in Unit #2. Annular gap measurement was done in Unit#1 before deployment of BARVIS during 25th Refuelling Outage (RFO) in Unit#1. Contrary to the expectation, the annular gap was found less and inspection of beltline region with BARVIS in Unit #1 could not be done. Finally during RFO in January 2016 of Unit #2, BARVIS has been successfully deployed for beltline region welds inspection. BARVIS mainly consists of manipulator, its operating system and data acquisition system. Data acquisition system and data analysis are not covered in this report.

Introduction

TAPS 1&2 are oldest operating plants built in 1960s. Assessment of RPV structural integrity is most important for ageing management and relicensing to extend safe operation of the reactor. RPV is comprised of shells and removable top head with flange & bottom head which is welded to shell and multiple nozzles & penetrations. Cylindrical vessel is made of three cylindrical shell courses each shell course has two longitudinal welds and then each shell course is joined together by circumferential welds. Shells are made of low alloy steel and clad with 5.56mm (7/32 inch) thick austenitic steel. Vessel internal diameter is 3657.6 mm (144 inch). It has total six longitudinal welds and four circumferential welds as shown in Fig. 1. The vessel welds are to be inspected periodically as part of regulatory requirement. Manipulators for inspecting welds from ID surface of RPV for Boiling Water Reactors (BWR) have been developed in past by GE for inspection - system GERIS 2000 [1] and RPV-Inner Diameter (ID) scanner [2]. These manipulators are big in size and provide circumferential and longitudinal scanning movements to the probes independent to the fuelling bridge. During weld inspection of RPV of TAPS-1&2, drier and separator assemblies are removed from the RPV top shell. As a result upper shell welds L1-1, L1-2 and their junctions with C1 become accessible for inspection from ID side. A simple and compact size Weld Inspection Manipulator [3] has been used for upper shell welds inspection at TAPS-1&2.

Inspection of middle shell (beltline region) welds is extremely difficult. Direct accessibility of welds from ID is hindered by core internals (thermal skirt, sparger, core spray sparger pipes etc) as shown in Fig. 2. C2 weld is located behind the thermal skirt which is not accessible from ID. However, beltline longitudinal (L2-1, L2-2 welds and their junction with C3) welds are accessible through a limited annular gap of 25 mm between RPV wall and thermal shield. Core spray sparger pipes makes the task more challenging as the location of L2-1 & L2-2 welds are

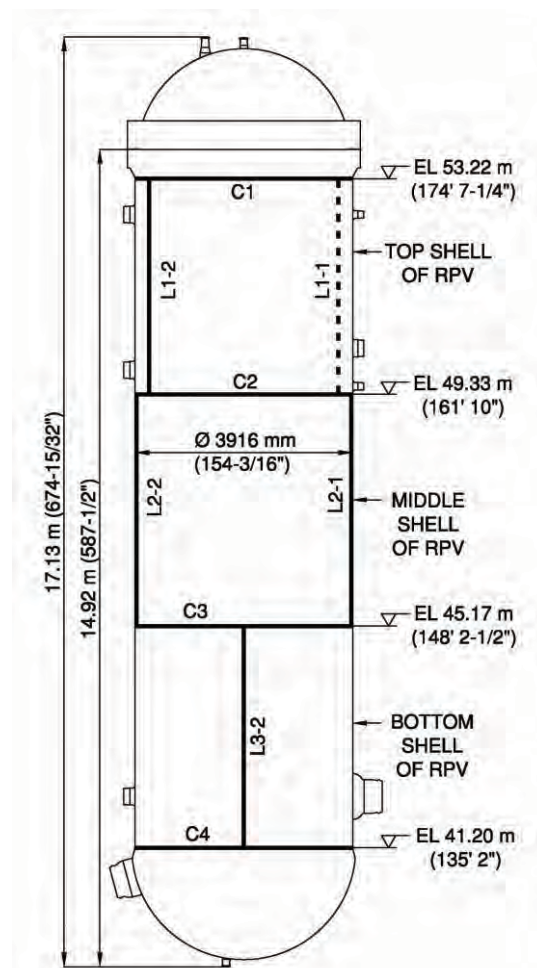


Fig. 1: Schematic of Reactor Pressure Vessel

exactly behind these pipes. Newer generation of BWRs have more gaps between RPV wall and thermal shield and are designed considering In-Service Inspection of RPV [2]. Inspection of RPV beltline regions welds of BWR/1 which have very small annular gap from ID is not attempted worldwide.

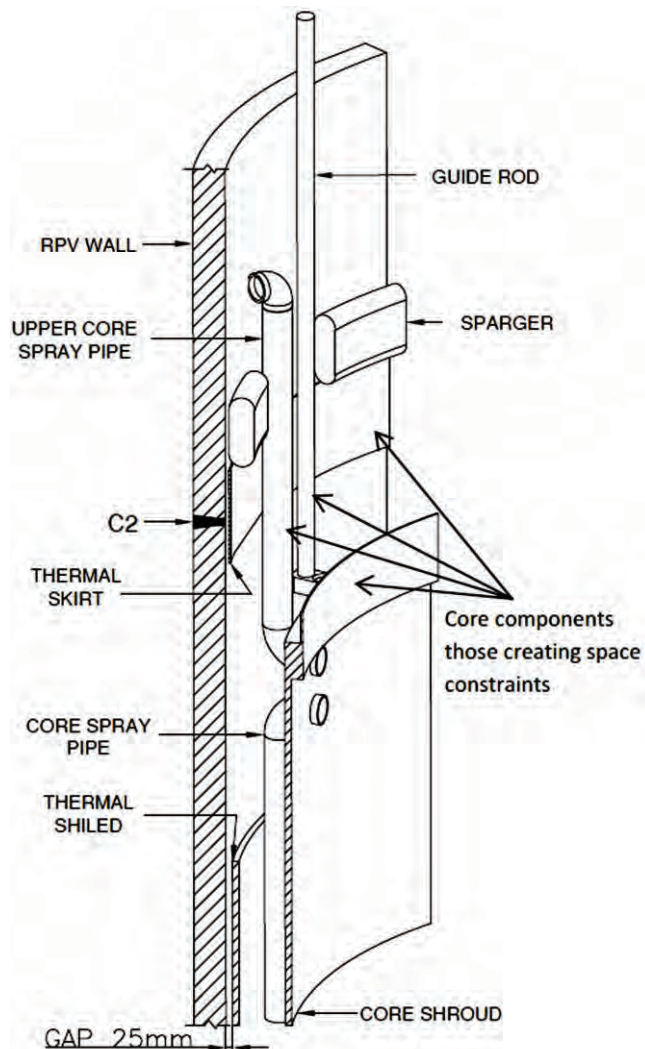


Fig. 2: Schematic Details of RPV Internals

BARVIS is designed to address this challenging inspection task for beltline region welds of TAPS-1&2. BARVIS mainly consists of manipulator, operating control panel, UT&ECT probes and data acquisition. Ultrasonic & ECT methods, probes, data acquisition and analysis are not in the scope of this report. This report describes design of manipulator and its operation only.

General Description & Working principle: During weld inspection vessel top head is in open condition and the dryer & separator are removed from the RPV. Reactor cavity is filled with water and the grapple of refuelling bridge is available to handle the manipulator which is placed at parking stand in reactor cavity with the help of over head crane. Bail on the top of manipulator is similar to the fuel assemblies. Grappler picks up the manipulator from parking stand and places it on to the top of core shroud as shown in the Fig. 3. Manipulator

location on the core shroud is fixed by pin guided in to the hole in the bracket welded to core shroud similar to dryer & separator assembly and takes lateral support from the separator guide rod which is fixed to the RPV. Manipulator is further clamped to guide rod by cylinder actuated grip named here as monkey grip.

For covering weld inspection from both side of the centre line of the welds and Heat Affected Zone (HAZ), probe holder associated with chain drive assembly is swung to avoid core spray pipe obstruction. After inspection of first weld, manipulator is picked up by grapple and is installed at other similar weld location (180° opposite to first weld) on the top of core shroud. Manipulator provides continuous vertical movement of 4000mm (speed 25 mm/s) which covers up to C3 weld junction, indexed cross travel of 500mm at top and 80mm cross travel at probes for scanning/cleaning weld joint and HAZ. Vertical movement to the probes/brush is provided by push pull chain. Circumferential/cross movement is provided by lead screw & nut. Indexed cross movement is restricted by separator guide rod in one side (only 150 mm travel from centre of weld) and obstructed by core spray pipe on other side. To avoid obstruction, the probe holder/brush is provided with swinging movement. After clearing obstruction, further cross movement of 250 mm in other side of the centre of weld is available. This cross movement is sufficient to scan the full weld and HAZ.

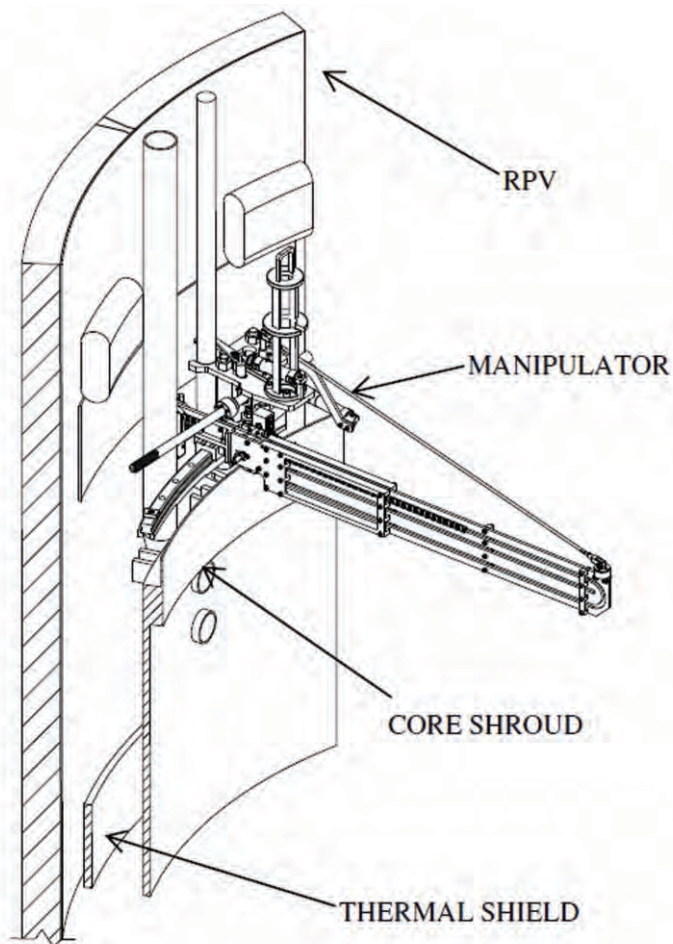


Fig. 3: Manipulator mounted on top of Core Shroud

Four different types of end-effectors (surface cleaning brush, horizontal scanning probe holder-1&2 and vertical scanning probe holder) can be assembled to the manipulator as shown in the Fig. 4 with horizontal probe holder. Initially, manipulator will be assembled with surface cleaning brush. Brush is pushed to the cladded surface by magnetic force and then vertical up/down motion is provided by chain. For cleaning full inspection surface the brush is indexed in steps of 50mm by the cross movement. Indexed cross movement is done when the linear rigid chain is in fully retracted condition.

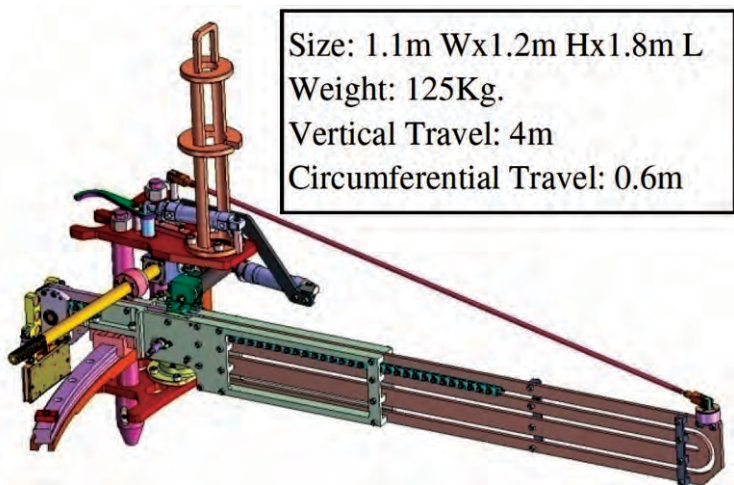


Fig.4: 3D Schematic of Manipulator attached with horizontal probe holder

Detail Design:

The weld inspection manipulator has to perform five important functions namely: (i) anchoring to the reference point and providing vertical up/down movement to the probe holder/cleaning brush (ii) circumferential motion of probe holder or weld cleaning brush across the HAZ (iii) Scanning surface cleaning (iv) UT & ECT scanning of welds and (v) swinging operation to avoid core spray pipe obstruction. Accordingly there are five major subassemblies to perform these functions: (a) support structure (b) Indexed cross travel & vertical travel sub assembly (c) Probe Holder Cross travel assembly (d) Probe holder sub-assemblies (i.e. horizontal scanning, vertical scanning, brush etc), (e) Operating Software.

Support Structure

Support structure (see Fig. 5) provides mounting & locating features to install at core shroud inside RPV. Support structure houses curved rail for providing indexed cross travel, cylinder for swinging to avoid obstruction of core spray sparger pipe and monkey grip to fasten with guide rod. Support structure is made up of top & bottom plates, support & locating rods for fixing in to core shroud, bail suitable to grapples for handling, curved rail for cross travel pivoted in end for swinging, swing cylinder and anchor axle for tie rod. Bottom plate rest on the sitting collar of separator made in core shroud and have features to mount swing axle hosing and support & locating

rods. Top plate have feature to mount bail, swing cylinder bracket, anchor axle housing etc.

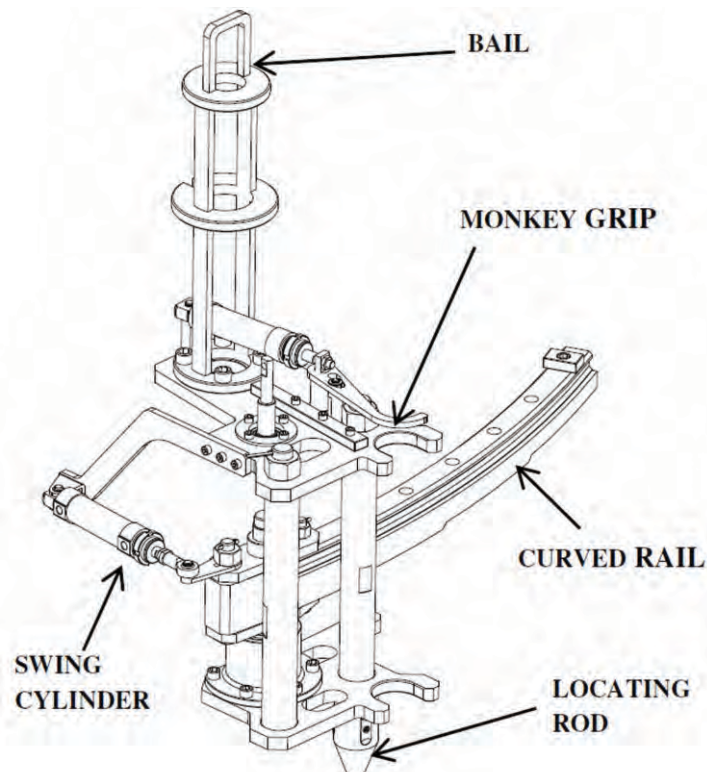


Fig. 5: Support Structure SA

Lead Screw & Nut SA

This consists of lead screw & nut, bearings housing, air motor for driving screw and potentiometer for measuring cross travel as shown in the Fig. 6. Screw housing is pivoted on the curved rail and the nut is pivoted on the LM block to provide free rotation to follow the curvature of the rail. Lead screw is 30mm in diameter and 6mm pitch. It is driven by low rpm air motor (rated torque 20 Nm@ 25rpm).

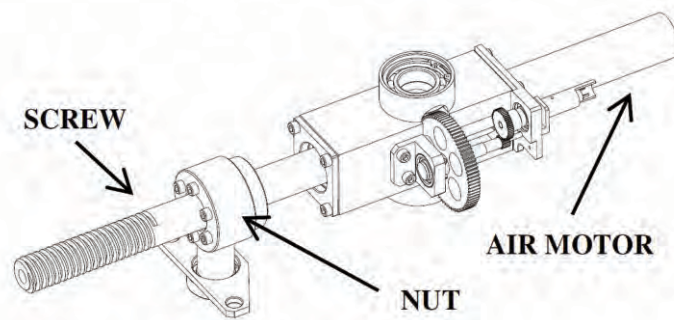


Fig. 6: Support Structure SA

Cross & Vertical Travel SA

Push pull chain as shown in Fig.7 is used to provide vertical up/down movement to the probes/brush. Direct chain coming out from the standard chain sprocket assembly could not be used to provide vertical motion as the width of the standard sprocket assembly and drive unit is more which restrict the travel between the separator guide rod and the core spray sparger pipe.

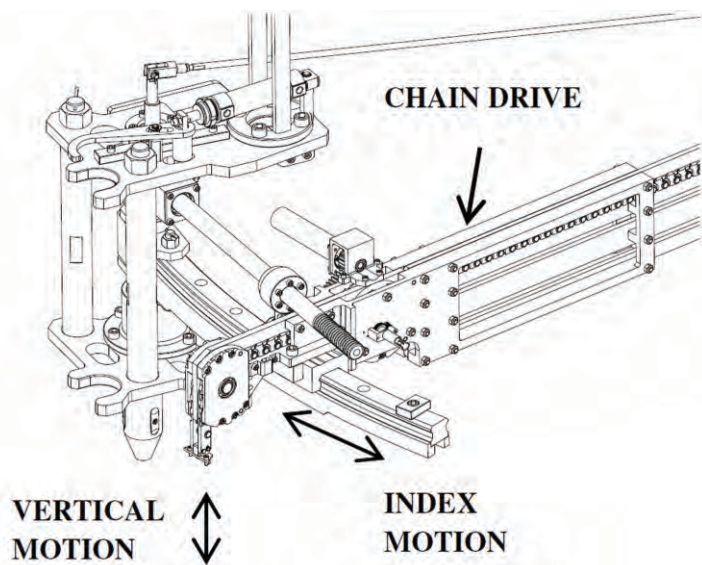


Fig. 7: Cross & Vertical Travel SA

Vertical motion to the probes/brush is managed by combination of reduced width idler sprocket assembly and the customized standard chain drive sprocket assembly. Chain width is also reduced to 22mm from standard 23.5mm to pass through into annular gap with clearance. Chain sprocket is driven by air motor through reduction to provide linear speed of inspection ranging from 4mm/s to 25 mm/s. A 10 turn potentiometer similar to cross travel is mounted on other side of sprocket to measure accurately the vertical position with reference to top of core shroud.

Horizontal Scanning Probe Holder

Horizontal Scanning Probe holder (see Figs. 8&9) which has front face curvature matching to the clad surface of RPV and back face curvature matching with outer surface of shield with clearance is made of two sub assemblies i.e. probe holder base and probe holder.

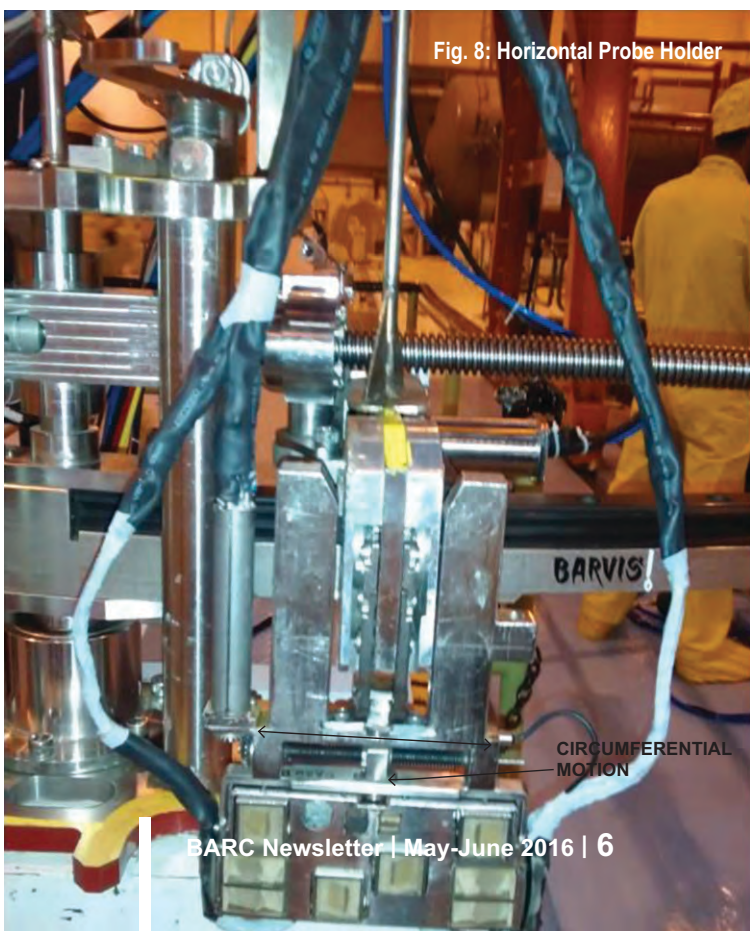


Fig. 8: Horizontal Probe Holder

Probe holder base consists of magnets, cross travel drive mechanism, cross travel sensing mechanism and spring supported idler wheel assembly. Probe Holder base is connected to the chain. Probe holder which houses 8 nos. of UT probes and ECT probe is connected to the screw nut of base assembly for cross travel movement. Magnets are used in base to adhere to the RPV ID surface. In addition to magnetic attraction force idler wheel assembly also pushes the probe base towards the RPV wall in annular gap by taking support from thermal shield. Idler wheel assembly also helps in restricting swinging movement of the probe holder while travelling down. Probes are spring supported and have two degree of freedom to overcome undulation in the inspection surface while maintaining the proper contact. Cross travel movement to the probe holder with respect to base is achieved by nut and screw mechanism driven by pneumatic motor. A normal beam UT probes is used for position feedback. Probe is fixed to the base and the time of the reflected ultrasound beam from the target mounted to the moving nut is calibrated for distance. To cover weld centre and HAZ by all angled probes and the normal beam, there are two type of horizontal scanning probe holders.

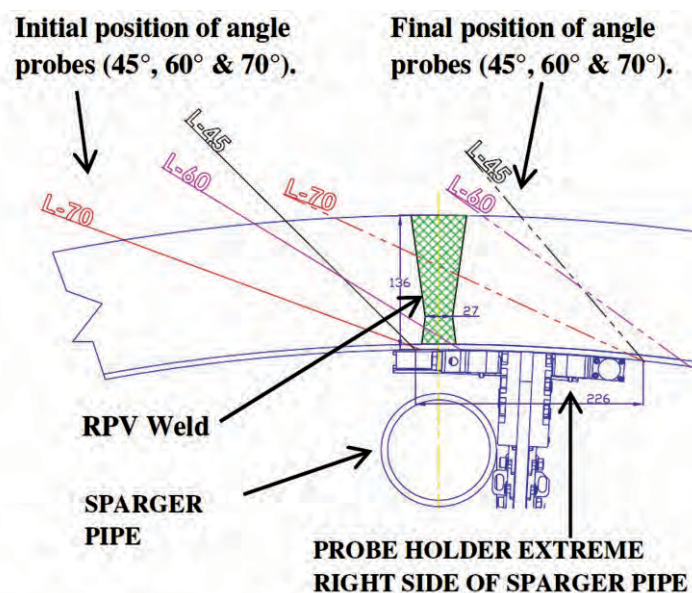


Fig. 9: Schematic of inspection coverage by left side probes in right side of sparger pipe

Vertical Scanning Probe Holder

Vertical probe holder is connected to the chain in similar way as horizontal probe holder and holds same no of probes (see Fig. 10). Probes are mounted such that beam path of upper row of angled probes is scanning upward and bottom row probes beam path is scanning downwards. Vertical probe holder needs only vertical movement and indexed cross travel for scanning. It does not require cross travel movement at probe holder. It also houses magnets and spring supported idler wheel assembly for pushing probes towards RPV ID surface

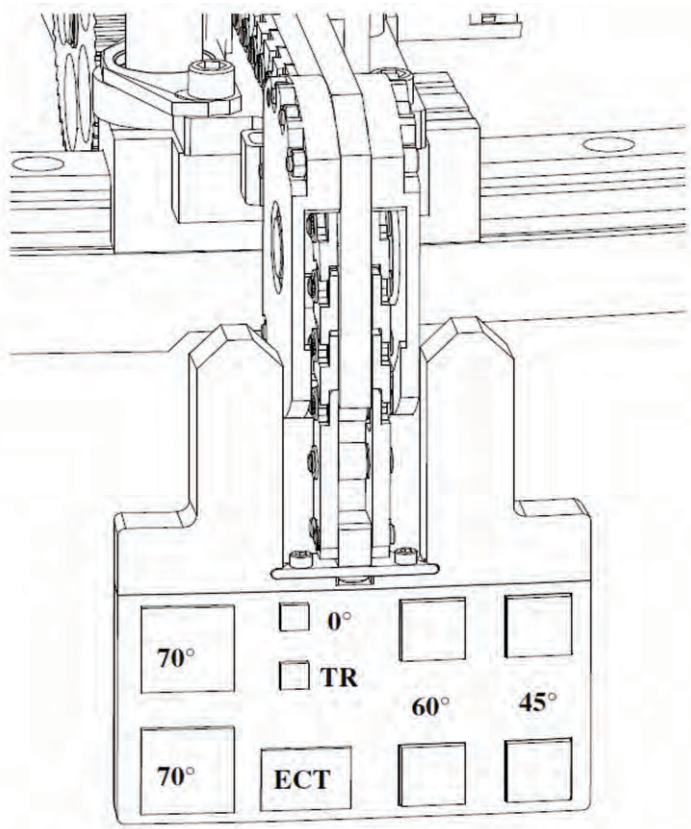


Fig. 10: Vertical Scanning Probe Holder

Cleaning Brush

Cleaning brush (see Fig.11) is a simple rectangular shaped having nylon bristled of 5-6mm length. Its base width is 22 mm. Brush is attached in front of push pull chain similar to



Fig. 11 Cleaning brush

probe holder. Its bristles are pushed towards the RPV wall by magnetic attraction towards RPV wall. The brush is moved up/down along the weld and indexed by cross travel to clean the inspection area. Magnets housed in top and bottom base of brush provides radial attraction force for cleaning the surface while moving vertically up/down by chain.

PC based Automation and Control Scheme

The control scheme is designed to facilitate safe and reliable operation of the system from remote panel located on 200 feet elevation floor near the Fuelling Machine Bridge. A PC based Graphical User Interface (GUI) M-SOFT is developed to make operation easier and more operators friendly as shown in Fig.12. The system operation consist mainly five motions to be controlled remotely i.e. chain up/down movement, cross travel movement, cross travel index movement, monkey grip cylinder and swinging (rotary motion to avoid obstruction of probes with core spray sparger pipe).

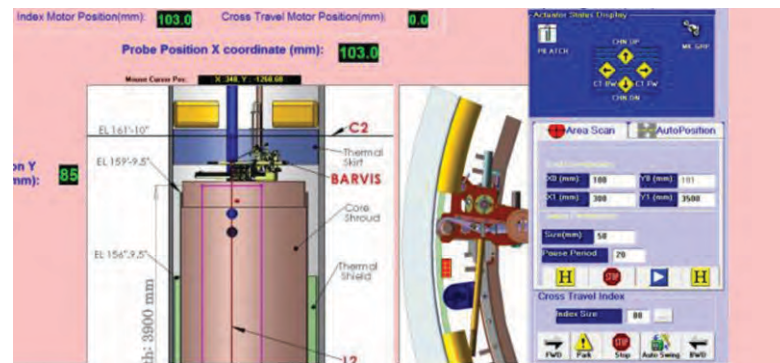


Fig. 12 Graphical User Interface (GUI)

A USB based data acquisition system is used to acquire potentiometer signals from actuators as well as provide 24V on/off signals to solenoid valve through relay contacts. The potentiometer signals are processed through control logic programmed in personnel computer in order to display position in value as well in graphical format. Algorithm developed to provide functionality like Auto Swing Operation, Auto-position operation, Auto Area scan sequence for horizontal and vertical mode of scan. The potentiometer signals are also connected to UT probe data acquisition system in parallel. All hardware (including pneumatic valves) is mounted on a free standing enclosed IP32 protected operator console. Field signals from field are connected to the Data Acquisition System through detachable industrial type connectors.

An indigenous developed UT flaw detector developed by Electronics Division, BARC is used to acquire UT probe data. Position information of probes is acquired from potentiometers in parallel. During Area Scan operation both systems are required to communicate each other for proper scanning. The control system facilitates this communication through digital input/output of the data acquisition card.

Testing & Qualifications:

A test set-up (see Fig. 13) is designed for performance testing of Manipulator. Test set up consists of a sector of simulated RPV shell, calibration block having weld overlays and notches and RPV internals. Simulated RPV shell sector is made by rolling of a carbon steel plate of same diameter as the RPV (154-3/16 inch) in outer diameter but 6 mm thick. A 6 mm thick SS 308 plate is rolled and attached to ID of this shell to simulate the RPV cladding. Core internals are provided to simulate obstructions. Annular gap between core shroud and RPV wall is closed for filling water. Carbon steel plate shell simulating RPV contains a number of standard notches of predetermined orientation and location.



Fig. 13: Manipulator mounted on Test setup

Performance testing of manipulator was carried out in the shop as well as in AAFR building at TAPS. At AAFR test setup was immersed in water. The 500 mm band containing defects was scanned using Manipulator and the results (see Fig. 14) were co-related with manual scanning data. Horizontal probe holder, cleaning brush and operating panel being tested on test set up are shown in the Figs. 15, 16&17.

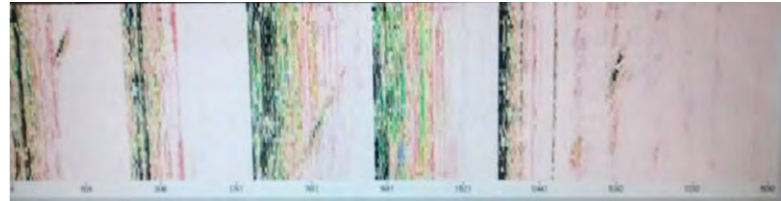


Fig. 14: Area scanning results



Fig. 15: Horizontal Probe holder entering in the annular gap of test set up



Fig. 16: Inspection Surface Cleaning

During qualification trials at AAFR, several modifications were carried out in the BARVIS to improve the performance of scanning. Some of the important modifications are mentioned here. Horizontal probe holder design was changed to accommodate higher frequency probes and to provide more degree of freedom to the probes for better contact. Cross travel position feedback was changed from potentiometer to UT based distance measurement. Mounting base plate of the manipulator was re-machined to ease in installation on top of core shroud.

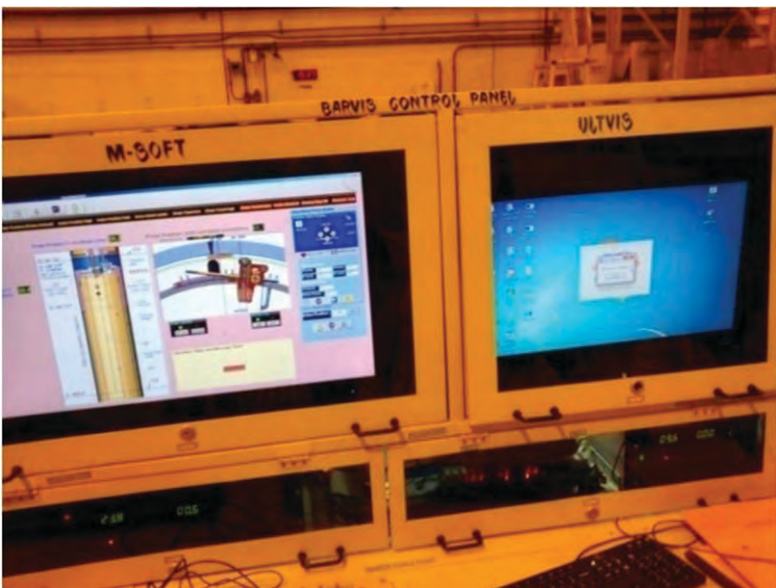


Fig. 17: Control Panel

Deployment in the Reactor:

Annular gap measurement was done in Unit#1 before deployment of BARVIS during 25th RFO in Unit#1. Surprisingly, annular gap was found less and inspection of beltline region with BARVIS in Unit#1 could not be done. Finally during RFO in January 2016 of Unit #2, BARVIS (as shown in Fig. 18) has been successfully deployed for beltline region welds inspection.



Fig. 18: Manipulator Parked on Stand



Fig. 19: Manipulator Lifted by crane

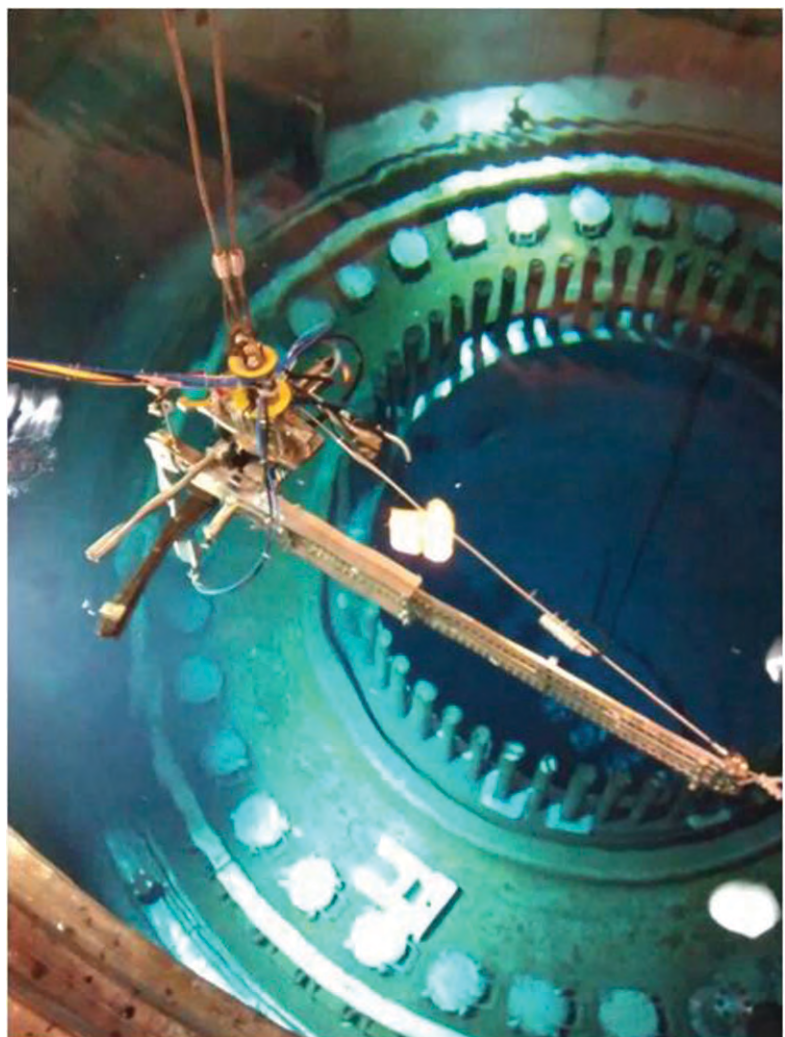


Fig. 20: Manipulator lowered on to stand



Fig. 21: Picked up by Grappler from stand

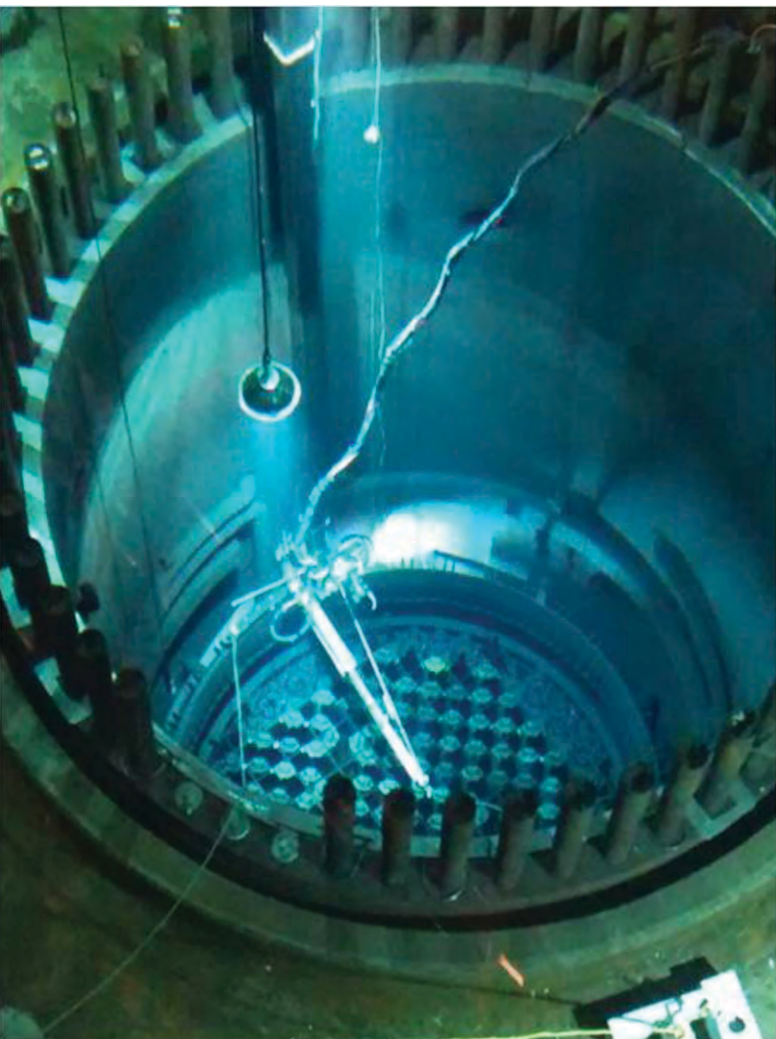


Fig. 22: Manipulator anchored and ready for weld inspection



Fig. 23: Performing Weld Inspection



Fig. 24: Probe Holder entered in to the annular gap

In this unit, inspection was done only up 2600mm from the reference against as planned 3800mm due to non availability of the clear annular gap beyond 2600. HAZ were cleaned by weld cleaning brush. UT scanning of these welds was successfully carried out. Inspection of one longitudinal weld joint with one type of probe holder in core region takes average 30 hrs. There are total four attachments i.e. one cleaning brush, two horizontal probe holders and one vertical probe holder to complete the inspection of one weld. Deployments photographs in sequence of operation are shown in the figs. 19-24.

Conclusion:

BARVIS has been deployed successfully during current outage in TAPS-2 in January 2016. Firstly, area to be scanned along the longitudinal welds, on either side of the weld joints, was cleaned satisfactorily using brush by making up/down movement and indexed travel. Subsequently BARVIS was deployed for inspecting the welds in both vertical & horizontal direction. UT & ECT examination data was acquired by NDT experts and presently being reviewed.

Development and deployment of BARVIS is first of its kind which has enabled the cleaning and inspection of welds in core region first time in 45 years of operation. This timely development has helped NPCIL to meet the commitments of core welds inspection which was considered earlier to be impossible.

Acknowledgment

Authors would like to thank colleagues from BARC and Site who provided NDE & Data acquisition support without whom deployment of BARVIS could not have been successful.

References:

1. Dykes E R, "An advanced ultrasonic system for BWR vessel weld inspection", Nuclear Engineering and Design 148 (1994), P101-108.
2. Koch D and Molpeceres D, "Non-Intrusive BWR Reactor Pressure Vessel Inner Diameter", Inspection Scanner, 6th International Conference on NDE, October 2007, Budapest, Hungary.
3. H Chatterjee, JP Singh, R Ranjon, MP Kulkarni, RJ Patel, "Design & Development of Weld Inspection Manipulator for Reactor Pressure Vessel of TAPS-1", BARC newsletter, Issue no 330, 2013.

Atomic Dynamics and Anomalous Thermodynamic Behavior of Novel Compounds

R. Mittal, M. K. Gupta, S. K. Mishra, Prabhasree Goel and S. L. Chaplot

Solid State Physics Division

We discuss recent advances in modeling of anomalous thermodynamic properties using the techniques of lattice dynamics and scattering experiments. Our work on negative thermal expansion (NTE) in several compounds provided understanding of the underlying mechanism. Specific anharmonic phonons have been identified that are responsible for NTE in terms of translation, rotation and distortion of atomic polyhedral units. Our studies on vibrational and thermodynamical properties of lithium-based superionic conductors provide a correlation between lithium diffusion and dynamical instability. Extensive studies on multiferroic and perovskite materials enable to understand the role of phonon instabilities and their correlation to structural distortions, leading to phase transitions in these compounds.

Keywords: Phonons, Inelastic neutron scattering, Ab-initio, Phase transition

Introduction

Many macroscopic physical properties like phase transition, thermal expansion, specific heat and many others depend on the microscopic motion of various atoms inside a solid. Such collective and coherent motion of atoms forms travelling waves known as lattice vibrations. These vibrations are quantized in energy; the quantized vibrations are termed as "Phonons". In insulators, where there are no free electrons, phonons play a vital role in determining the elastic, dielectric, optical and thermodynamical properties. To have a microscopic level understanding of solids, it is important to probe its structure and dynamics. Structure can be determined by various diffraction techniques while dynamics can be studied by inelastic scattering of light, X-rays or neutrons, etc.

Unlike Raman scattering and infrared absorption, which essentially probe only the long wavelength phonons, inelastic neutron and X-ray scattering can directly probe the phonons of all wavelengths in the entire Brillouin zone. Experimental studies at high pressures and temperatures are often limited and accurate models for theoretical studies of various materials are of utmost importance. For this purpose, theoretical studies based on lattice dynamical methods are necessary for exploring the entire spectrum of thermal vibrations in crystals. The experimental data is used to validate the theoretical models. Once a model is validated successfully, this may further be used to predict the thermodynamic properties at various thermodynamical conditions. We have used the state of the art classical and density functional theory methods to compute the total energy and forces, and hence the phonons in entire Brillouin zone for various compounds. To validate the theoretical

results, the inelastic neutron scattering experiments have been performed. We have studied [1-13] variety of oxide materials to understand the role of phonons in their functional properties like negative thermal expansion, superionic conduction, multiferroicity etc. The motivation for studying the various compounds and significant results from some of our work are discussed below.

Negative Thermal Expansion Behaviour

During the last two decades anomalous or negative thermal expansion (NTE) has been reported in many frame-work solids. We have been investigating [2-5] these compounds to understand the underlying mechanism. Here we summarize the results obtained from our studies [3] on M_2O ($M=Ag, Cu$ and Au) compounds.

The compounds M_2O crystallize in a simple cubic lattice. The M atoms are linearly coordinated by two oxygen atoms, while oxygen is tetrahedrally coordinated by M atoms. Ag_2O shows a large isotropic negative thermal expansion (NTE) over its entire temperature range of stability, i.e. up to ~ 500 K, while Cu_2O only shows a small NTE below room temperature. We have performed inelastic neutron scattering measurements of the phonon energy spectrum of Cu_2O (Fig. 1 (a)) and Ag_2O , and ab-initio density functional theory (DFT) calculations of all the three metal oxides (i.e. M_2O with $M = Au, Ag$ and Cu). The Grüneisen parameters are calculated from the volume dependence of phonon energies ($\Gamma = -\partial \ln E / \partial \ln V$) in the entire Brillouin zone, which are then used for computing the thermal expansion behavior (Fig. 1(b)). The calculated thermal expansions of Ag_2O and Cu_2O are negative, in agreement with available experimental data, while it is found to be positive for Au_2O .

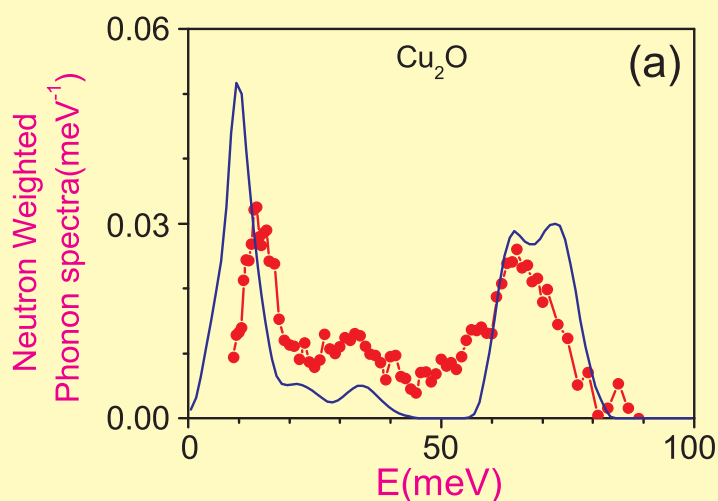
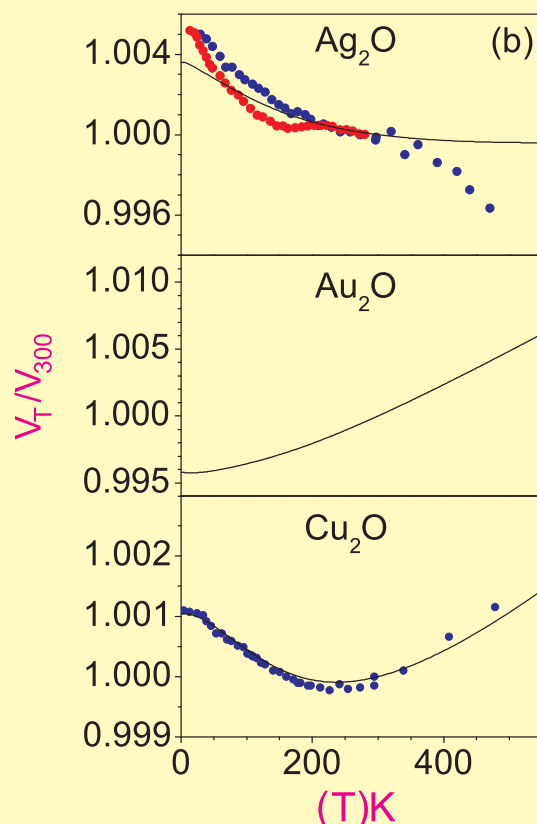


Fig. 1: (a) Experimental (symbols plus line) [4] and calculated (solid line) [3] neutron-weighted phonon spectra of Cu_2O . (b) The calculated (solid line) and experimental volume thermal expansion [3] of M_2O ($\text{M}=\text{Ag}, \text{Au}$ and Cu). The blue and red circles correspond to the experimental data from Tiano et al [14] and Kennedy et al [15] respectively. V_T and V_{300} are the cell volumes at temperatures T and 300 K, respectively



The nature of the low energy phonon modes contributing to the NTE can be visualized through animations [3] of lattice vibrations. The eigenvectors of a selection of them have been plotted on Fig. 2. The Γ (0,0,0), X ($\frac{1}{2}, 0, 0$), M ($\frac{1}{2}, \frac{1}{2}, 0$) and R ($\frac{1}{2}, \frac{1}{2}, \frac{1}{2}$) refer to specific points in the Brillouin zone

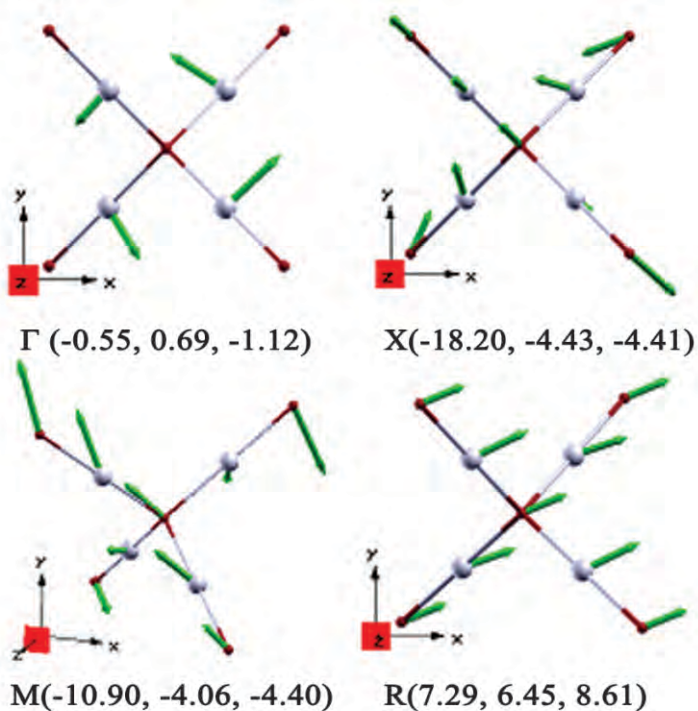


Fig. 2: Selected lattice vibrational modes [3] in M_2O ($\text{M}=\text{Ag}, \text{Au}$ and Cu), which contribute to the negative thermal expansion as calculated from ab-initio density functional theory. The numbers after the wave vector (Γ , X, M and R) give the Grüneisen parameters of Ag_2O , Au_2O and Cu_2O respectively. The lengths of arrows are related to the vibrational amplitudes of the atoms. Key: M, grey spheres; O, brown spheres.

corresponding to different wavelengths. The lowest-energy long-wavelength (Γ -point) optic phonon corresponds to the rotation of M_4O tetrahedral. The lowest energy X-point phonon involves bending of M-O-M chains. In this phonon the various M atoms forming an M_4O tetrahedron have different displacements indicating significant distortion of the tetrahedron. This phonon seems to contribute maximum to NTE in Ag_2O . The M-point phonon involves rotation, translation as well as distortion of the M_4O tetrahedra, while for R-point phonon the amplitude of all the atoms is similar and it indicates translational motion of M_4O as a rigid unit.

The compounds Ag_2O and Au_2O have nearly identical lattice parameters ($\text{Ag}_2\text{O} = 4.81 \text{ \AA}$ and $\text{Au}_2\text{O} = 4.80 \text{ \AA}$) and similar Ag/Au-O bond lengths. We show that the nature of chemical bonding and open space in the unit cell are directly related to the magnitude of thermal expansion coefficient. In order to understand the nature of the M-O bonding we have calculated the electronic charge density for the three compounds. We find that the bonding character of the Ag-O bond is more ionic than that of the Cu-O bond. We find that the Au-O bond is highly directional with the charge density elongated towards the O atom *i.e.* indicating a covalent nature. However, the covalent and directional Au-O bond rigidifies the Au_4O tetrahedra, making them less susceptible to distortion, bending or rotation than their Ag_4O counterpart. This reveals the microscopic origin of the large NTE in Ag_2O .

Now if we compare the Cu_2O and Ag_2O cases, for which the nature of bonding is very similar, we find that both the compounds exhibit negative thermal expansion at low

temperatures. However there is a large difference in the magnitude of the thermal expansion coefficient. The Cu-O (1.87 Å) bond length is much smaller than the Ag-O (2.08 Å) bond. The Cu₄O tetrahedral units are therefore much more compact than Ag₄O, rendering distortion less favorable in Cu₄O as compared to Ag₄O. The difference in the open space in the unit cell between the two compounds leads to differences in the magnitude of the distortions and hence difference in the NTE coefficient.

Superionic Diffusion and Phonon Instability

The performance of energy storage devices depends crucially on the properties of their component materials. An excellent example of innovative materials science is the discovery of the rechargeable lithium battery. The materials research [6, 7] based on computational methods now plays a vital role in characterizing and predicting the structures and properties of complex materials on the atomic scale.

Lithium oxide is a superionic material that exhibits high ionic conductivity above 1200 K. In this case, Li ions are the diffusing species, while oxygen ions constitute the rigid framework. At ambient conditions Li₂O occurs in the anti-fluorite structure. Oxygen ions are arranged in a face-centered-cubic sublattice with lithium ions occupying the tetrahedral sites. We have calculated the phonon spectrum using ab-initio density-functional theory and the generalized gradient approximation. The calculated phonon dispersion relation [6] at relaxed lattice parameter $a = 4.57 \text{ \AA}$ (at 0 K) is in good agreement (Fig. 3) with reported experimental data. The compound exhibits superionic transition in the vicinity of 1200 K. Hence we have performed phonon calculations at

various unit cell parameters corresponding to high temperatures. As expected, the phonon frequencies are generally found to soften with increase of volume. The softening is found to be small for all the phonon modes except for the lowest transverse acoustic (TA) branch along the [110] direction at Brillouin zone boundary. The eigenvector of the TA phonon has been plotted (Fig. 4(a)) corresponding to the unit cell parameter of $a = 4.88 \text{ \AA}$. We find that the lithium atoms in alternate layers move opposite to each other along [001] while oxygens are at rest. Hence increasing the temperature could lead to migration of lithium ions from one site to another vacant site along [001] direction, which can easily be visualized from Fig. 4 (a). The change in the TA phonon frequency (Fig. 4(b)) with increasing lattice parameter shows that the lowest TA phonon along [110] at zone boundary softens sharply at volume corresponding to the superionic regime. At the superionic transition, some of the lithium atoms might just have sufficient energy to move from their ideal positions and start diffusing. It is possible that the softening of these phonons might be the precursor to the process of diffusion.

Phase Transitions in Multiferroic Perovskites

The interest in perovskite-like oxides continues for decades because of many attractive phenomena observed in these compounds. Among them are structural phase transitions, ferroelectricity high- T_c superconductivity, colossal magnetoresistance, charge and orbital ordering, complex magnetic properties, etc. Phonons play a vital role to understand the underlying physics [8-13]. For example, manganites, RMnO₃ ($R = \text{Dy-Lu, In, Y, and Sc}$), have been a subject of interest for

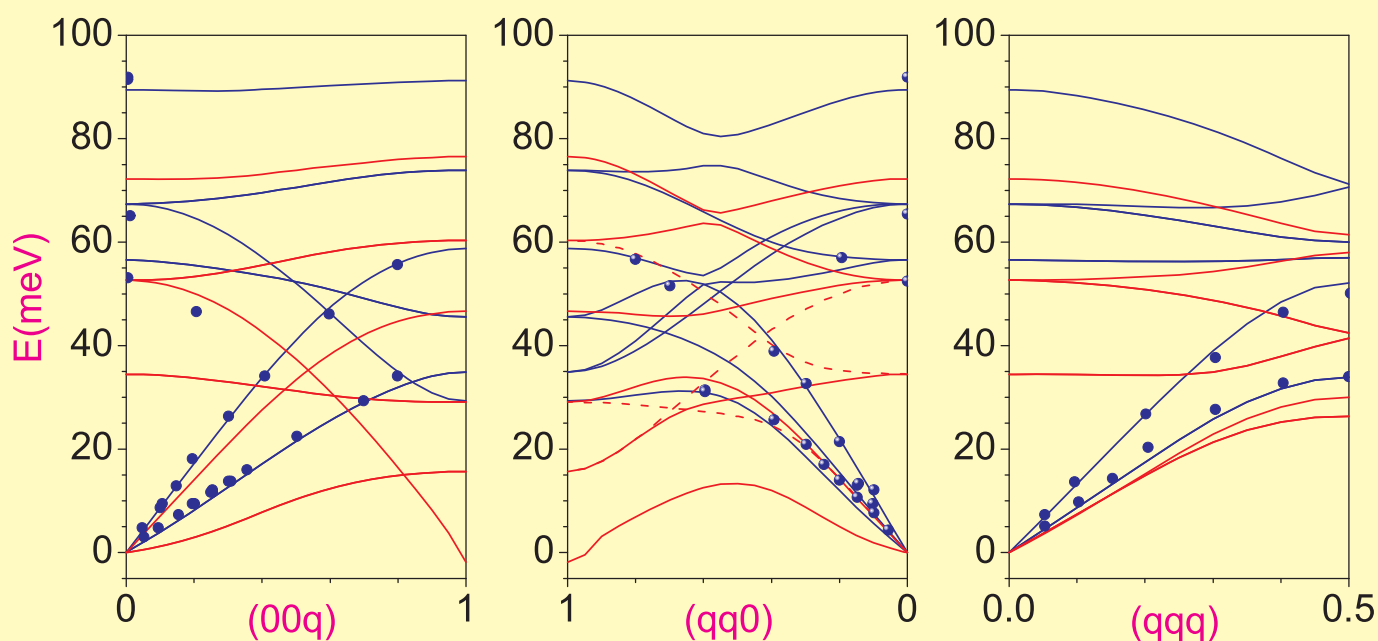


Fig. 3: Phonon dispersion relation from ab-initio density functional theory [6] under generalized gradient approximation (GGA). The blue and red lines correspond to calculations performed at $a = 4.57 \text{ \AA}$ and $a = 4.94 \text{ \AA}$ respectively. The solid symbols correspond to reported experimental [16] data at room temperature that may be compared with the calculations with $a = 4.57 \text{ \AA}$.

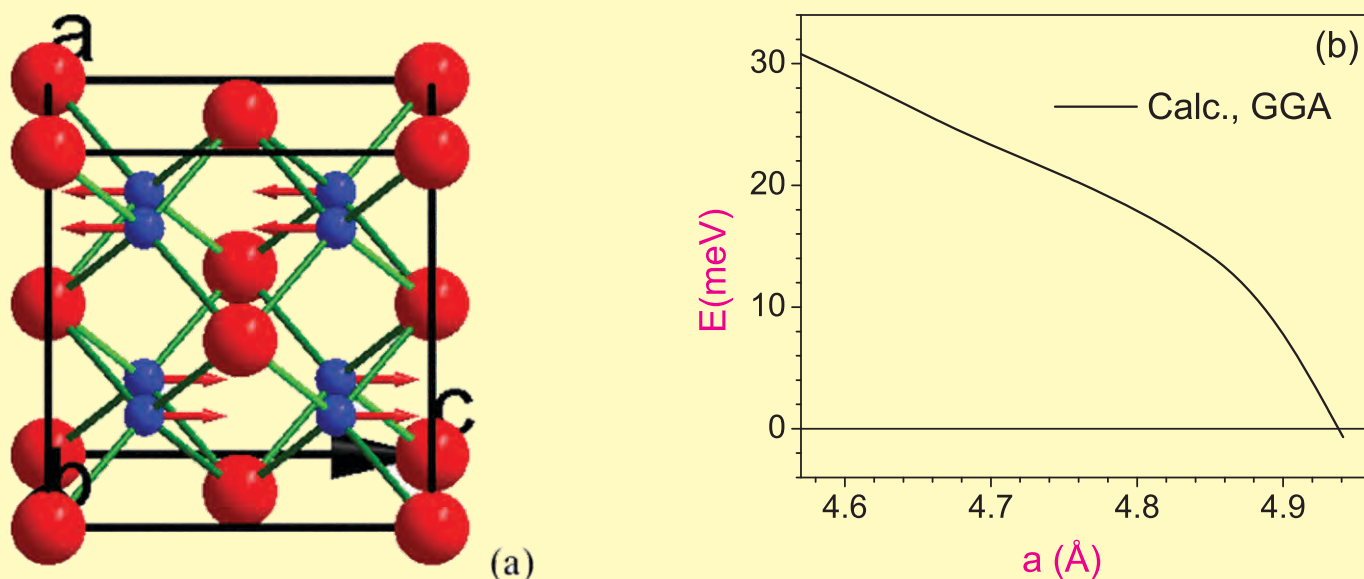


Fig. 4: (a) Vibrational pattern of individual atoms [6] for the zone boundary TA mode along [110] direction. Key; O: red spheres, Li: blue spheres. (b) Softening of the zone boundary TA phonon [6] along [110] with increase in the lattice parameter.

decades. These materials belong to a distinguished class of multiferroics, since they exhibit ferroelectricity and magnetism simultaneously.

Yttrium manganese oxide (YMnO_3) keeps attracting a keen interest as it is known to exhibit ferroelectricity and antiferromagnetism simultaneously. At ambient conditions the compound has a hexagonal structure with the space group $P6_3cm$. Above 1258 ± 14 K, a ferroelectric to paraelectric phase transition occurs, and the system crystallizes in a different hexagonal space group $P6_3/mmc$. We have carried out inelastic neutron scattering measurements on YMnO_3 . Measurements

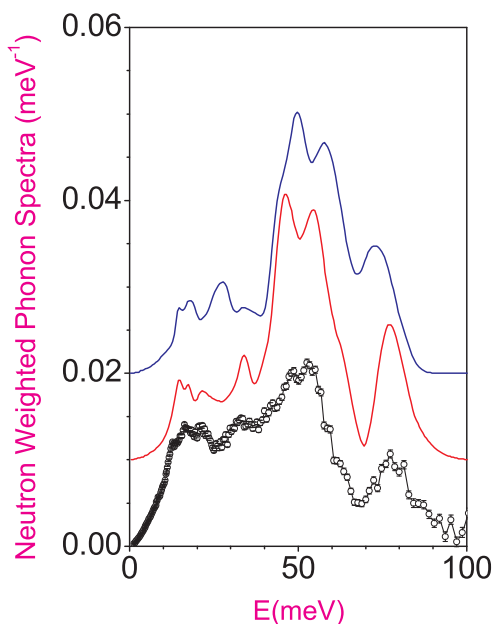


Fig. 5: The calculated (lines) and experimental (symbols joined by line) neutron inelastic spectra [9] of YMnO_3 . The red and blue lines correspond to the calculations performed with and without including the magnetic structure respectively. For better visibility, the experimental and calculated phonon spectra are shifted vertically with respect to each other.

are accompanied by ab-initio calculations of phonon spectra for the sake of interpretation and analysis of the measured phonon spectra. The experimental structure and the measured neutron inelastic spectrum are found (Fig. 5) to be better described by the ab-initio calculations when the magnetic structure is included, reflecting that the lattice couples to the magnetic structure.

Phonon dispersion relations in the entire Brillouin zone have been calculated [9] in both the high- and low-temperature hexagonal phases of YMnO_3 . The phonon modes in the low-temperature phase are found to be stable in the entire Brillouin zone. However, in the high-temperature phase phonon instability is clearly noticed at the high-symmetry wave-vector K ($1/3, 1/3, 0$). The unstable mode is highly anharmonic in nature, and it becomes stable at high temperatures due to anharmonicity. It has been proposed that the condensation of the unstable phonon mode at K point drives the transition to the low-temperature structure of YMnO_3 . It is found that this K -point mode is not a polar mode. However, ferroelectricity in YMnO_3 arises from the coupling of the unstable K -point mode with a stable mode at the Γ -point. The latter mode is polar in nature and, therefore, contributes to the ferroelectricity in the low-temperature phase. The eigenvectors of these modes have been extracted from our ab-initio DFT calculations. The atomic-displacement pattern of these modes is shown in Fig 6. At the K -point, the mode consists of an unequal displacement of two Y atoms in opposite direction, along with an out-of-phase rotation of MnO_5 bipyramid units around the c -axis. The unequal amplitude of the vibrations of the O atoms induces a distortion of the MnO_5 units. The displacement pattern of the stable mode at the Γ -point consists of vibration of O atoms belonging to the plane formed by the Mn atoms of the MnO_5 units.

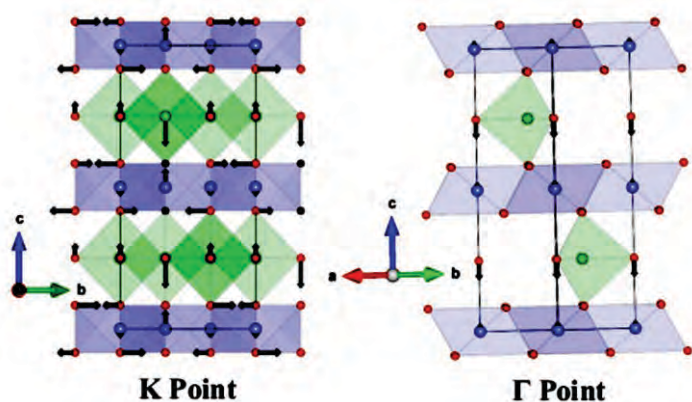


Fig. 6: The displacement patterns [9] of the lowest-energy phonon modes of wave-vectors at the K and Γ points in the high-temperature phase of YMnO_3 . The lengths of arrows are related to the vibrational amplitudes of the atoms. The absence of an arrow on an atom indicates that it is at rest. Key: Y, blue spheres; Mn, green spheres; and O, red spheres.

Conclusions

The work described here uses the techniques of lattice dynamics calculations and inelastic neutron scattering measurements to understand the thermodynamic properties of various compounds. The role of atomic vibrations in various thermodynamical properties like thermal expansion, specific heat, temperature- and pressure- driven phase transitions and ionic conduction in various compounds is explained.

References

1. R. Mittal, S. L. Chaplot and N. Choudhury, Modeling of anomalous thermodynamic properties using lattice dynamics and inelastic neutron scattering, *Progress in Materials Science* 51 (2006) 211
2. M. K. Gupta, R. Mittal and S. L. Chaplot, Negative thermal expansion in cubic ZrW_2O_8 : Role of phonons in entire Brillouin zone from ab-initio calculations, *Phys. Rev. B* 88 (2013) 014303.
3. M. K. Gupta, R. Mittal, S. L. Chaplot and S. Rols, Phonons, nature of bonding and their relation to anomalous thermal expansion behavior of M_2O ($\text{M}=\text{Au}, \text{Ag}, \text{Cu}$), *Journal of Applied Physics* 115 (2014) 093507.
4. R. Mittal, S. L. Chaplot, S. K. Mishra, and Preyoshi P. Bose, Inelastic neutron scattering and lattice dynamical calculation of negative thermal expansion compounds Cu_2O and Ag_2O , *Phys. Rev. B* 75 (2007) 174303.
5. M. K. Gupta, Baltej Singh, R. Mittal, S. Rols and S. L. Chaplot, Lattice dynamics and thermal expansion behavior in metal cyanides, MCN ($\text{M}=\text{Cu}, \text{Ag}, \text{Au}$): Neutron inelastic scattering and first principles calculations, *Phys. Rev. B* 93 (2016) 134307.
6. M. K. Gupta, Prabhathasree Goel, R. Mittal, N. Choudhury and S. L. Chaplot, Phonon instability and

mechanism of superionic conduction in Li_2O , *Phys. Rev. B* 85 (2012) 184304.

7. Prabhathasree Goel, M. K. Gupta, R. Mittal, S. Rols, S. J. Patwe, S. N. Achary, A.K. Tyagi and S. L. Chaplot, Phonons, lithium diffusion and thermodynamics of LiMPO_4 ($\text{M}=\text{Mn}, \text{Fe}$), *J. Mater. Chem. A* 2 (2014) 14729.
8. M. K. Gupta, R. Mittal, M. Zbiri, R. Singh, S. Rols, H. Schober and S. L. Chaplot, Spin-phonon coupling, high pressure phase transitions and thermal expansion of multiferroic GaFeO_3 : A combined first principles and inelastic neutron scattering study, *Phys. Rev. B* 90 (2014) 134304.
9. M. K. Gupta, R. Mittal, M. Zbiri, Neetika Sharma, S. Rols, H. Schober and S. L. Chaplot, Spin-phonon coupling and high-temperature phase transition in multiferroic material YMnO_3 , *J. Mater. Chem. C* 3 (2015) 11717.
10. Prabhathasree Goel, M. K. Gupta, R. Mittal, S. Rols, S. N. Achary, A. K. Tyagi and S. L. Chaplot, Inelastic neutron scattering studies of phonon spectra and simulations of pressure-induced amorphization in tungstates AWO_4 ($\text{A}=\text{Ba}, \text{Sr}, \text{Ca}$ and Pb), *Phys. Rev. B* 91 (2015) 094304.
11. S. K. Mishra, M. K. Gupta, R. Mittal, M. Zbiri, S. Rols, H. Schober and S. L. Chaplot, Phonon dynamics and inelastic neutron scattering of sodium niobate, *Phys. Rev. B* 89 (2014) 184303.
12. Preyoshi P. Bose, M. K. Gupta, R. Mittal, S. Rols, S. N. Achary, A. K. Tyagi and S. L. Chaplot, Phase transitions and thermodynamic properties of Yttria, Y_2O_3 : Inelastic neutron scattering shell model and first-principles calculations, *Phys. Rev. B* 84 (2011) 094301.
13. S. K. Mishra, M. K. Gupta, R. Mittal, A. I. Kolesnikov and S. L. Chaplot, Spin-phonon coupling and high pressure phase transitions of RMnO_3 ($\text{R}=\text{Ca}$ and Pr): An inelastic neutron scattering and first principle studies, *Phys. Rev. B* 93 (2016) 214306.
14. W. Tiano, M. Dapiaggi and G. Artioli, Thermal expansion in cuprite-type structures from 10 K to decomposition temperature: Cu_2O and Ag_2O , *J. Appl. Crystallogr.* 36 (2003) 1461.
15. B. J. Kennedy, Y. Kubota, K. Kato, Negative thermal expansion and phase transition behaviour in Ag_2O . *Solid State Communications* 136 (2005) 177.
16. S. Hull, T.W.D. Farley, W. Hayes and M.T. Hutchings, The elastic properties of lithium oxide and their variation with temperature, *J. Nucl. Mater.* 160 (1988) 125.

Phase distribution study for U-Zr-metallic simfuel

S. Kolay, M. Basu, S.N. Achary and A.K. Tyagi

Chemistry Division

D. Das

Raja Ramanna Fellow-Chemistry Group

S. Kaity and J. Banerjee

Radiometallurgy Division

A detailed study of the phase evolution in a U-10wt%Zr alloy fuel simulated with fission products corresponding to 10 atom% burn-up and annealed at 700° and 1000°C in vacuum is carried out by using XRD and microscopic techniques like SEM and EDS. The studies revealed segregation of major phases like bcc-U, -U and U_2Zr . SEM studies revealed the presence of segregated phases in the bulk matrix of uranium. Salient results are presented in this article.

1. Introduction

Nuclear power is an alternative currently available to supply enough energy to bring down global CO_2 level and this would require efficient harnessing of nuclear resources. The inception of nuclear technology took place with an all-metal fuel concept with liquid metal coolant reactors (LMRs) [1], obviously for the advantages like well-known chemical and physical behavior of metals and their alloys, ease of fabrication, simpler and smaller core designs, production of artificial fissile ($^{239}Pu/^{233}Th$) material inventory along with excellent neutron economy, high burn-up capability with inherent safety features and straightforward recycling by techniques like electro-refining. The emergence of the concept of integral fast reactor (IFR) is consociated with the recognition that the ^{238}U reserve of world must be efficiently utilized as an energy source in the centuries to come. Thus, the fuel system must be able to utilize plutonium as its principal fuel and must have the potential to simultaneously create plutonium by breeding ^{238}U . However, the low melting temperatures of pure plutonium and pure uranium-plutonium alloys makes it impractical to design a commercially viable reactor using only these elements. Several elements like Cr, Mo, Ti and Zr have been considered as additives for increasing the melting temperature. Out of these elements Zr is unique, since it enhances the compatibility of fuel and SS clad by suppressing the inter-diffusion between them. By the end of 1960s, 10 wt% of zirconium and 20 wt % of plutonium alloy fuel (remaining uranium) with satisfactory fuel-clad compatibility and raised solidus temperature had been developed.

The appropriate selection of alloy fuel is closely linked with their metallurgical characteristics along with

other thermo-physical and neutronic characteristics. The metallurgical properties of alloy fuel systems, like the binary alloys of plutonium and zirconium with uranium as base matrix have been extensively studied. U-Zr binary alloy is an important sub-system of the U-Pu-Zr ternary alloy which provides alternate choices of alloy fuels. U-rich Zr alloys are known to exhibit excellent corrosion resistance and dimensional stability during thermal cycling. Based on irradiation experiments, the alloy U-10 wt% Zr has been proposed as a prospective fuel for fast breeder reactors [2]. A number of reports are available in literature on properties of Zr-rich U-Zr alloys [3, 4] and U-rich U-Zr alloys [5-7]. Broadly, these studies indicate the formation of saturated alpha-U type phase in U rich region while gamma (bcc) or hexagonal (δ) type phase in Zr rich regions. Also, it has been observed that hexagonal (δ) U_2Zr_2 type phase precipitates on annealing the alloys.

Based on the literature information, it can be concluded that the virgin fuel itself can give rise to a wide variety of microstructures depending on composition and thermal history. Moreover, the porosity and microstructure of U-Zr alloy are strongly dependent on the composition and phases of the alloy. The porosity also influences the extent of fuel swelling and gas release which affects the integrity and performance of fuel. Thus it is desirous to know the phase evolution of a fuel subjected to a sufficiently high burn-up. Such fuel contains myriads of fission products along with alloying elements. This situation generates several phase fields due to interaction of base matrix elements and fission products and this leads to phase segregation induced structural changes in the microstructure of fuel assembly. Reported information shows successful performance of alloy fuel with the porous matrix in achieving 10-15 atom % burn-up [8]. With an aim to generate

information on phase and micro-structural changes in high burn up conditions, a detailed study of the phase evolution in a U-10wt%Zr alloy fuel simulated with fission products corresponding to 10 atom% burn-up and annealed at 700° and 1000°C in vacuum is carried out by using XRD and microscopic techniques like SEM and EDS. The salient results are presented in this article.

2. Experimental

U-rich U-Zr alloys (U-10 wt%Zr) were prepared by melting appropriate amounts of elements in an arc melting furnace in an inert (Ar) atmosphere. Oxygen impurity in the flowing Ar gas was removed by passing it over hot uranium turnings. The alloy buttons thus obtained were re-melted 3-4 times to ensure chemical homogeneity. Prior to incorporation of the noble metal fission products (Pd, Ru, Rh, Mo) in the parent alloy button they were reduced in 8%H₂-Ar at 700°C for 3 h to remove any oxide impurity present. After this treatment, calculated amounts of Pd, in form of small wire pieces, and Ru, Rh and Mo as powders (obtained from integrated fission product yields of natural uranium corresponding to 10 atom% burn-up) were added to the parent alloy button and melted in arc melting furnace several times for homogenization. To a portion of this simulated alloy calculated amounts of Nd and Ce pieces (preserved in oil) were added and re-melted in arc melting furnace. The schematic of preparation of alloys of various compositions and their annealing protocol are shown in Fig. 1. The composition of the alloy with respect to the incorporated fission products (g/10g of natural U) is: Ru (0.9257), Rh (0.2551), Pd (0.5544), Mo (0.8667), Nd (0.9851), Ce (0.7418).

For the micrographic and XRD studies the alloys were cut into small pieces using slow speed diamond coated cut-off wheel. Standard metallographic procedures were followed for grinding and polishing. A small piece of the alloy was electro leached using aqueous solution of 50% H₃PO₄ as electrolyte and SS304 as cathode with a standard potential of 2 V. Micrographic characterizations were carried out using scanning electron microscope (SEM). The compositional analyses were carried out by energy dispersive spectroscopy (EDS). The same set of experiments was carried out at 1000°C with a separate set of alloys.

3. Characterization of phases

3.1. XRD studies

Initially all the XRD patterns were compared with the known phases of U and other compound phases (Fig. 2). The identification of phases from their corresponding XRD patterns were carried out by considering structure types known for different phases of U alloys. Since exposure area of sample in diffraction experiments is 0.5 x 0.5 mm, they provide the average existing bulk information. The change in focus spot on sample did not reveal any significant change in the diffraction patterns. Thus only the major phases could be identified by the XRD studies. The details of analyses of different samples are explained below.

The XRD pattern of the as cast alloy shown in Figure 2 indicates significantly broadened Bragg peaks. The analyses of the peaks were carried out by comparing the reported standard XRD patterns of known alloys or elements used as constituents. The absence of alpha-U can be ascertained in all the samples as can be seen from Fig. 2. It needs to be

mentioned here that the XRD peaks cannot be simply assigned to the known phase, due to the usage of diverse elements. Thus the analyses were carried out by considering various lattice types and typical unit cell parameters of the assigned phases. From the positions of intense peaks, two distinct stabilized bcc phases with unit cell parameters $a = 3.40$ and 3.33 \AA could be suggested for sample E (Fig. 3a). Both position and intensity of the intense peaks can be accounted by these two bcc phases. In addition, a monoclinic U₂Ru type (JCPDS-PDF 18-1145) and a tetragonal (β -U) [10] phase could also be

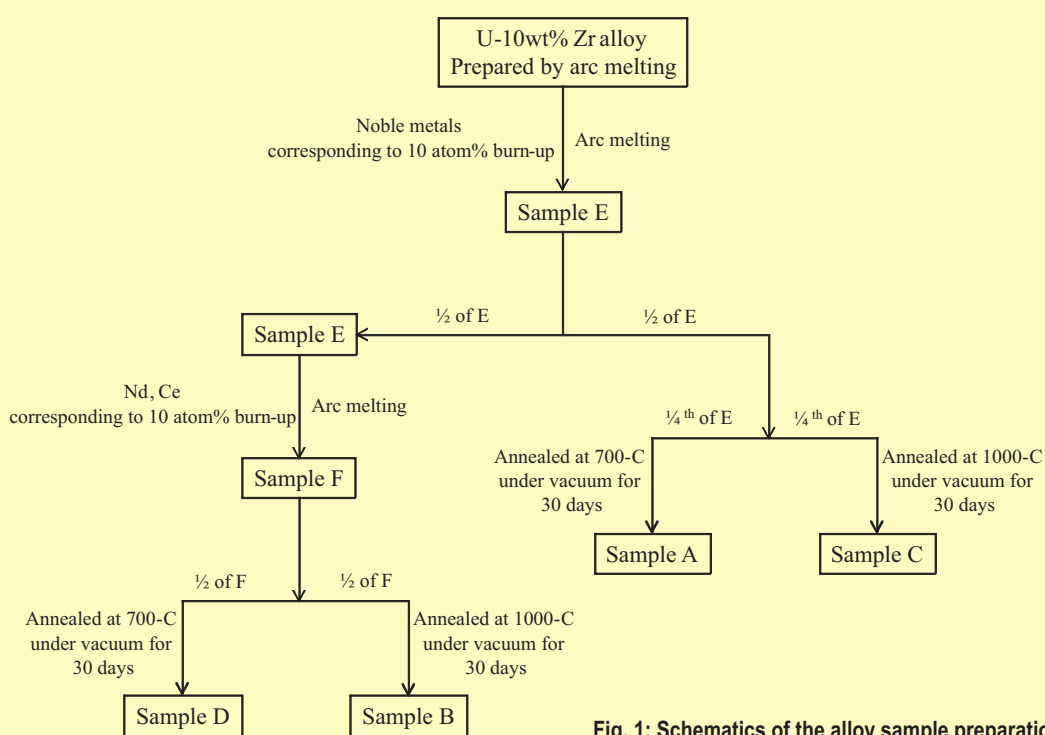


Fig. 1: Schematics of the alloy sample preparation

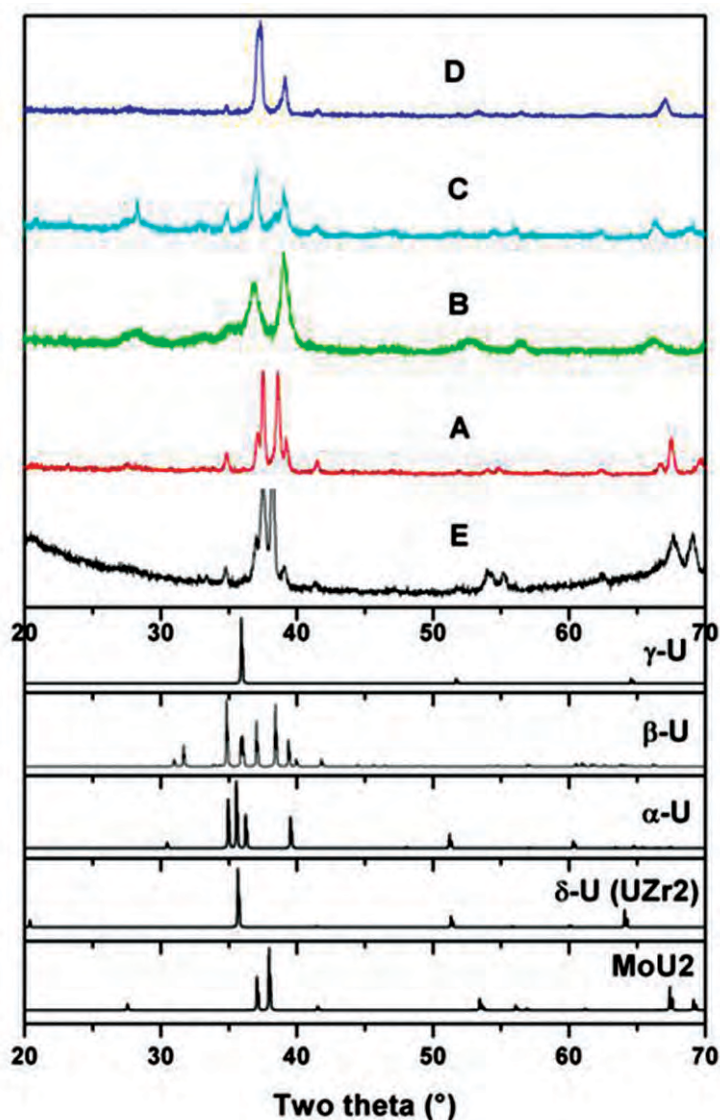


Fig. 2: Comparative XRD plots of our samples (A-E), -U [9], -U [10], -U [11], U-(UZr₂) [12] and U₂Mo [JCPDS-PDF file 12-0296]

identified from the observed peaks. Most of the observed peaks in XRD pattern could be explained by considering these four phases.

No hexagonal δ phase (UZr₂) phase [12] could be observed in this XRD pattern. As mentioned, each of the stabilized bcc phases of U may have some solubility of the added elements. The stabilization of bcc phases with Mo, Ru and Zr etc elements is known for uranium. Further the peak positions attributed to U₂Ru type phase and β -U phase are also not strictly matching with their reported unit cell details. Thus solubility of some added elements in these lattices also cannot be ruled out. No clear identification for the noble metals could be ascertained from this XRD pattern, which may be due to their insignificant contribution in the exposed area in XRD experiments or masking by the dominating peak of U-containing phases.

XRD patterns of sample A and D, the lower temperature (700°C) annealed U-Zr alloy containing noble metals and U-Zr alloy containing noble metals and rare-earth elements respectively, shown in Fig. 4a and 4b, are distinct from all other samples. In the sample D, the presence of bcc U phase ($a = 3.41$

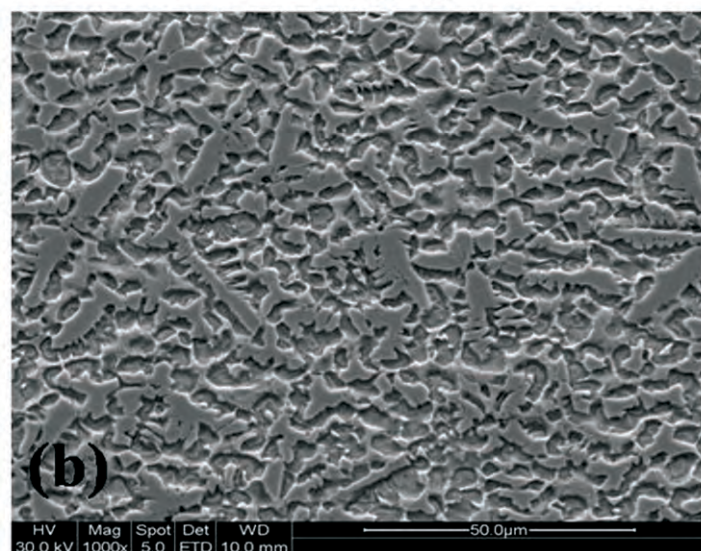
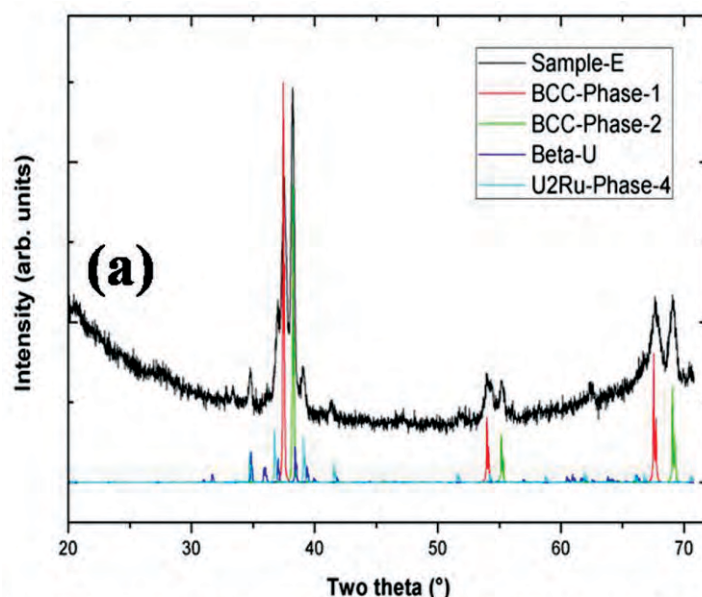


Fig 3: (a) XRD pattern of sample E (b) SEM picture of U-Zr alloy with noble metals (as-cast-Sample E)

Å) is clearly observed in the XRD pattern (Fig 4b). However, the presence of monoclinic U₂Ru type phase may also be suggested from the peak position at 34.8° and 41.5°. A closer analysis of the peak at 37.2° indicates splitting, which might be due to composition heterogeneity of the bcc phase of U. Considering the multiplets of the 37.2° peak, this sample may have total three types of cubic phases, with unit cell parameters as: 3.43, 3.41 and 3.26 Å, respectively. Similar analyses of the XRD pattern of Sample-A (Fig 4a) revealed the presence of two types of bcc-U phases ($a = 3.40$ and 3.39 Å). The appearance of peaks at 34.8° and 41.5° suggests the presence of U₂Ru type monoclinic phase. However most of the peaks expected for U₂Ru type monoclinic phase are not observed. Some of the peaks could be attributed to -U and a feeble amount of fluorite type UO₂ phase can also be guessed from the broad peak at 28.1° (JCPDS-PDF 78-0725)

A simple comparison of the XRD patterns (Fig 4d and 4c) of high temperature annealed (1000°C) alloys, namely sample B (U-Zr alloy containing noble metals and rare-earth elements) and sample-C (U-Zr alloy containing noble metals) indicates

some similarity. In both the XRD patterns the bcc phase of U could be identified. In contrast to sample-B, where two types of stabilized bcc phases exist, the sample C shows only one type of bcc phase. The peaks attributable to bcc phase in sample B could be assigned to $a = 3.46$ and $a = 3.32$ Å, while the identified bcc phase in sample C has unit cell parameter: $a = 3.44$ Å. This difference can be due to redistribution of elements at higher temperature. The unit cell parameters observed for sample C might be due to incorporation of elements of wider atomic radii.

It may also be important to note that broad overlapping peak like features are observed at the positions of -U (Cmcm), [11] in sample B (inset in Fig. 4d). However no clear information can be obtained due to poor peak shapes in this XRD pattern. Further it can be noticed that in both sample B and C, U_2Ru type monoclinic phase is observed. Thus the sample C has only one stabilized bcc phase which probably disintegrates in sample B, due to additional constituent elements (such as Nd and Ce). The observed U_2Ru type phase does not show much difference in these two XRD patterns. The segregation of elements may be a reason for the appearance of the -U phase. Also, a broad hump or peak observed at two-theta $\sim 29^\circ$ in the XRD pattern of both B and C may be due to surface oxidation of uranium metal to fluorite type UO_2 phase (JCPDS-PDF 78-0725).

3.2. Contrast and microstructure studies by SEM-EDS.

The SEM micrograph of sample E (as-cast alloy of U-Zr containing noble metals) shows almost uniform microstructure with different contrast indicating the presence of one each of U-rich Zr deficient and U-deficient-Zr-rich phases (Fig. 3b, Table 1). This is different from the fine lamellar structure present in U-10wt%Zr as-cast alloy with a single phase as reported in literature [13]. This observation is in accordance with the XRD results. Though the microstructure appears close to that reported for UZr_2 type phase [12], the absence of corresponding peaks in the XRD pattern (Fig. 3a) excludes its existence. No distinct contrast for -U and U_2Ru , as identified by XRD, is seen in the SEM micrograph.

Table 1: EDS analyses results (as atom fraction) of U-Zr + Noble metals as-cast alloy

As-cast			
Grey part		Base matrix	
Element	Atom Fraction	Element	Atom Fraction
U	0.08	U	0.52
Zr	0.5	Zr	0.04
Ru	0.14	Ru	0.08
Rh	0.04	Rh	0.008
Pd	0.16	Pd	0.04
Mo	0.06	Mo	0.3

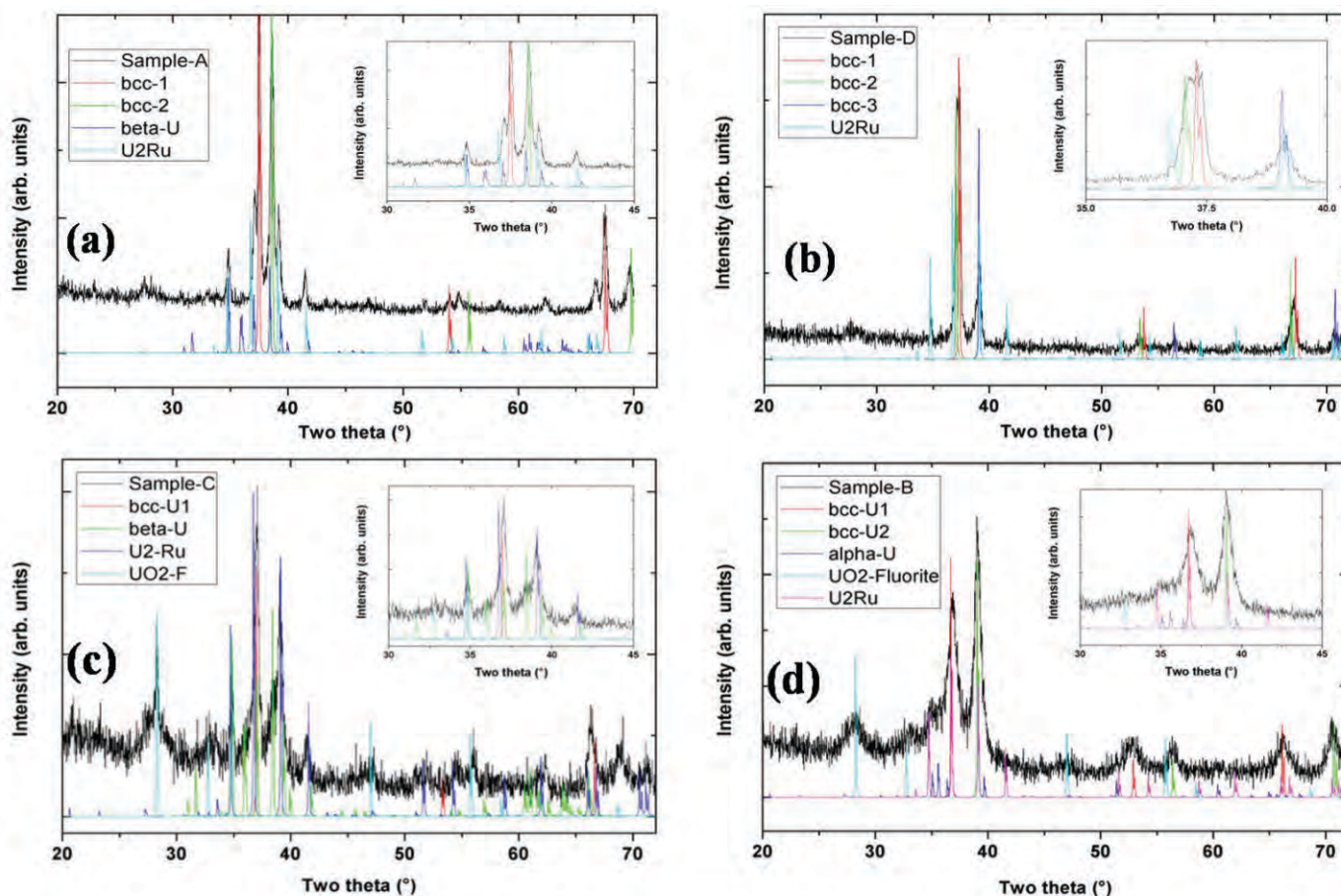


Fig. 4: XRD patterns of sample-A (a), sample-D (b), sample-C (c), sample-B (d)

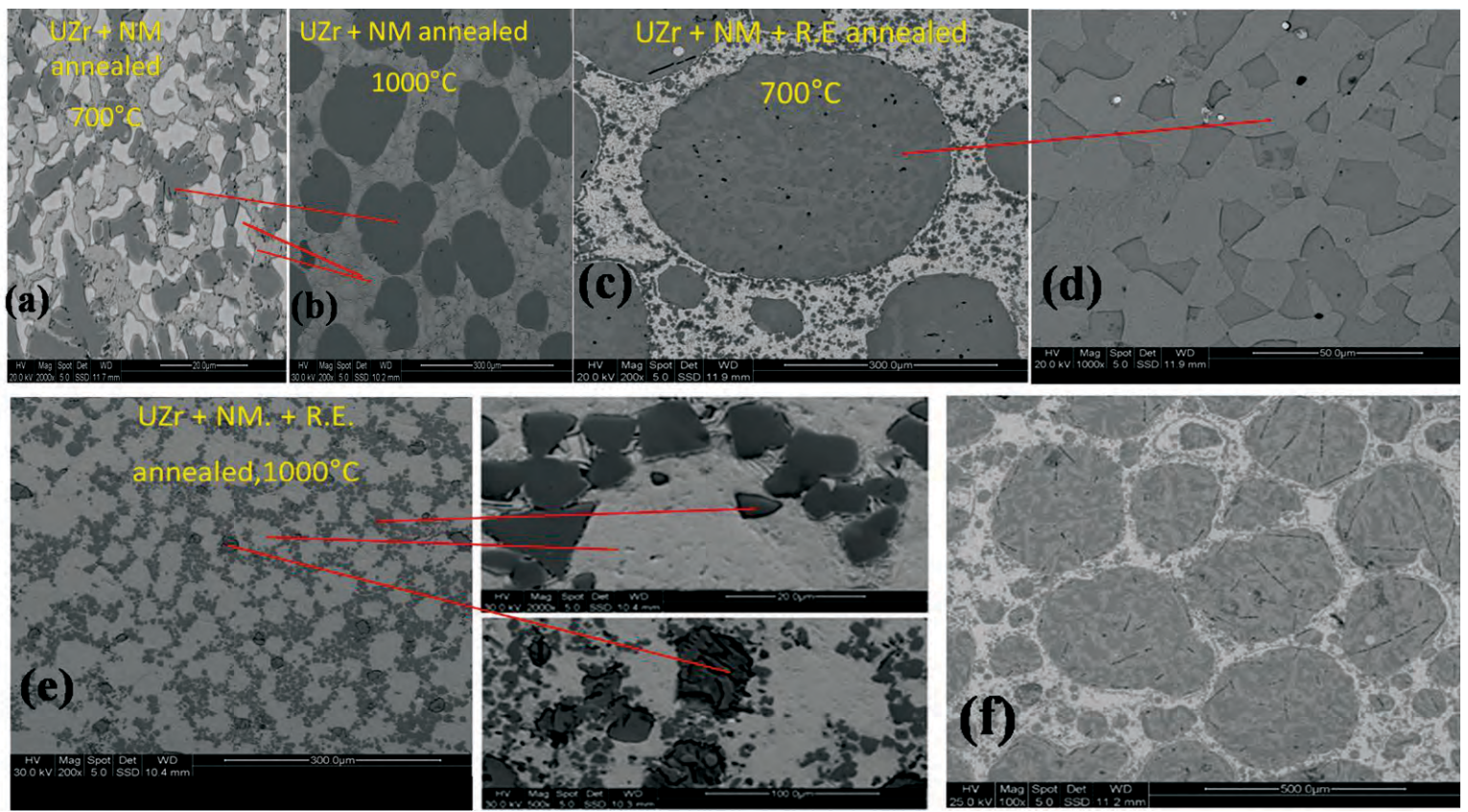


Fig. 5: SEM pictures of sample-A (a), sample-C (b), sample-D (c, d), sample-B (e) and U-Zr-NM-RE-as-cast alloy (f)

The sample A, which is obtained by annealing the alloy containing noble metals at 700 °C shows segregation of different phases with different contrast like white, light grey and dark regions (Fig-5a). The EDS analyses (Table 2) on the light phase show that it is U rich, Zr deficient with no Pd. The other two phases contain all the noble metals along with the parent components. The dark grey phase is richer in Pd and Mo than the lighter grey one. However, this noble metal containing phases could not be seen in XRD. The SEM micrograph of the sample C which is obtaining by annealing the alloy at 1000 °C shows two phase fields (Fig 5b). The original dark grey phase of the original alloy remains unchanged in their elemental composition during annealing at 1000°C. However, the white and light grey phases observed at low temperature annealing appear to merge into a grey

phase with needle shaped morphology. This phase is rich in Rh and Pd but deficient in Mo when compared to the corresponding phases in 700°C annealed sample (Table 2). The observed two phase type behavior indicates the presence of dark grey bcc-U phase and lighter grey U₂Ru type phase containing the Rh and Pd etc.

On addition of rare-earths elements, the distinct transformation of the microstructure of as-cast alloy into dark patches with intricate network structure and lighter region with four different phases having slightly varying contrasts is observed (Fig. 5f, Table 3). Significant changes are observed on annealing this alloy sample. The 700 °C annealed sample (sample D, Fig. 5c) shows two sharply contrasting regions: Dark patches and lighter regions having isolated phase precipitations. The dark patches are Pd, Nd and Ce rich

Table 2: EDS analyses results (as atom fraction) of U-Zr+Noble metals annealed alloys.

Elements	UZr matrix + Noble metals					
	700°C annealed			1000°C annealed		
	White region	Light grey	Dark grey	Grey needle	Grey matrix	Dark spot
U	0.73	0.6	0.15	0.65	0.3	0.1
Zr	0.017	0.011	0.35	0.03	0.01	0.39
Ru	0.02	0.27	0.15	0.15	0.19	0.18
Rh	0.009	0.05	0.05	0.02	0.04	0.08
Pd	0.0	0.019	0.19	0.04	0.02	0.19
Mo	0.22	0.04	0.10	0.08	0.01	0.06

Table 3: EDS analyses results (as atom fraction) of as-cast U-Zr + Noble metals + Rare-earth elements alloy

Elements	UZr matrix + Noble metals + Rare-earth elements					
	Dark patch			White matrix		
	Lighter region	Darker region	Spots	Lighter region	Darker region	Spots
U	0.004	0.006	0.006	0.7	0.25	0.17
Zr	0.0	0.03	0.03	0.05	0.29	0.11
Ru	0.0	0.2	0.02	0.08	0.15	0.17
Rh	0.03	0.06	0.05	0.01	0.03	0.31
Pd	0.51	0.30	0.33	0.009	0.01	0.20
Mo	0.0	0.0	0.0	0.14	0.27	0.01
Nd	0.29	0.31	0.28	0.0	0.0	0.006
Ce	0.15	0.27	0.27	0.0	0.0	0.017

Table 4: EDS analyses results (as atom fraction) of (U-Zr + Noble metals + Rare earth elements) alloy annealed at 700°C.

Elements	Dark spot		Base matrix			
	Lighter region	Darker region	White region	Light grey	Grey	Dark spots
U	0.008	0.004	0.77	0.42	0.16	0.02
Zr	0.008	0.03	0.02	0.20	0.40	0.08
Ru	0.0	0.02	0.04	0.30	0.31	0.05
Rh	0.026	0.11	0.0	0.04	0.046	0.36
Pd	0.52	0.27	0.0	0.0	0.0	0.36
Mo	0.0	0.0	0.17	0.03	0.08	0.01
Nd	0.27	0.28	0.0	0.0	0.0	0.03
Ce	0.16	0.28	0.0	0.0	0.0	0.08

Table 5: EDS analyses results (as atom fraction) of (U-Zr + Noble metals + Rare earth elements) alloy annealed at 1000°C

Elements	White matrix	Interconnected dark region	Isolated dark spots
U	0.686	0.017	0.010
Zr	0.021	0.455	0.019
Ru	0.133	0.422	0.092
Rh	0.009	0.042	0.266
Pd	0.046	0.003	0.500
Mo	0.097	0.061	0.015
Nd	0.002	0.00	0.053
Ce	0.004	0.00	0.045

(Table 4) and have platelet-like microstructures in the as-cast samples (Fig.5f). They get transformed to network like microstructure when annealed at 700 °C (Fig. 5d). The lighter region is a homogeneous distribution of four phases with varying proportions of the component elements as follows:

a) White region which is highly U-rich and moderately Mo-rich.

b) Light grey region which is U and Ru-rich with moderate amounts of Zr.

c) Grey region which is Zr and Ru rich with moderate amount of U.

d) Highly Pd and Rh rich grey spots. The XRD analyses of this sample showed presence of U₂Ru and bcc-U type phases.

The contrast variations might be due to different extent of substitution of other elements in both bcc and U₂Ru phases. On annealing this alloy to 1000°C (sample B) the alloy gets re-structured to three phases (Fig. 5e): A white U-rich region with moderate amounts of Ru, Mo and Zr, a Ru-rich grey region and Pd-rich grey spot-like phase precipitates containing moderate amounts of Rh, Ru and the rare-earths (Table 5), although XRD analyses indicates the presence of five phases. The reason for obtaining lower number of phase contrasts from micrographic analysis might be different pattern of distribution of noble metals and rare-earth elements into the basic lattices

4. Conclusion:

Phase distribution studies were carried out on U-10wt%Zr alloy simfuel using XRD and micrographic (SEM-EDS) techniques. The salient phase features of the annealed simfuel alloys deduced from these studies are as follows:

- i) U-Zr alloy containing noble metals and annealed at 700°C contain two bcc phases while the alloy with noble metals and rare –earth elements and annealed at 700°C contain three bcc phases. On annealing these respective alloys to 1000C the number of bcc phases get reduced to one and two, respectively. The observation of multiple bcc phases may be due to substitution of different elements to different extents leading to composition heterogeneity.
- ii) All the annealed alloys show the presence of monoclinic U₂Ru phase with dissolved noble metal or rare-earth elements in it.
- iii) Alloy containing only noble metals show the presence of additional phase like less-symmetric -U while the alloy with noble metals and rare-earth elements (1000 °C annealed) show the features similar to -U.
- iv) All the features observed in XRD of both as-cast and annealed samples are not observed in SEM and vice versa. This is probably due to lot of dissolution and re-distribution of noble metals and rare-earth elements amongst the main parent lattices.

References:

1. Horst K. M., "The LMFBR-An international effort". *IEEE Transactions on Power Apparatus & Systems*. PAS-97 (2), (1978) 529-535.
2. Walters, L. C., "Thirty years of fuels and materials information from EBR-II". *J. Nucl. Mater.* 270 (1999): 39-48.
3. Takahashi Y., Yamawaki M., Yamamoto K., "Thermophysical properties of uranium-zirconium alloys". *J. Nucl. Mater.* 154 (1988):141-144.

4. Takahashi Y., Yamamoto K., Ohsato T., Shimada H., Terai T., Yamawaki M., "Heat capacities of uranium-zirconium alloys from 300 to 1100 K". *J. Nucl. Mater.* 167 (1989):147-151.
5. Basak C., Prasad G. J., Kamath H. S., Prabhu N., "An evaluation of the properties of as-cast U-rich U-Zr alloys". *J. Alloys Compd.* 480 (2009):857-862.
6. Basak C., Keswani R., Prasad G. J., Kamath H. S., Prabhu N., Banerjee S., "Investigation on the martensitic transformation and the associated intermediate phase in U-2wt% Zr alloy". *J. Nucl. Mater.* 393 (2009):146-152.
7. Kaity S., Banerjee J., Nair M. R., Ravi K., Dash S., Kutty T. R. G., Kumar Arun, Singh R. P., "Microstructural and thermophysical properties of U-6wt% Zr alloy for fast reactor application". *J. Nucl. Mater.* 427 (2012):1-11.
8. Hofman G. L., "Irradiation behavior of experimental Mark-II Breeder Reactor-II Driver Fuel". *Nucl. Technol.* 47 (1980):7-22.
9. Huber J. G., Ansari P. H., "The super conductivity of bcc U-Zr alloys". *Physica B-C*, 135 (1985):441-444.
10. Tucker C. W., Senio P., "An improved determination of the crystal structure of -uranium". *Acta Crystallographica*, 6 (1953):753-760.
11. Chiotti P., Klepfer H., White R. W., "Lattice parameters of uranium from 25-1132°C". *Trans. Am. Soc. Met.* 51 (1959):772-786.
12. Akabori M., Itoh A., Ogawa T., Kobayashi F., Suzuki Y., "Stability and structure of the phase of U-Zr alloys". *J. Nucl. Mater.* 188 (1992):249-254.
13. Basak C., "Phase transformations in U-Zr alloy system". *BARC Newsletter*, issue no 316 (Sep-Oct) 2010:60-64.

Acknowledgement

We thank Dr. S. Khan, Glass and Advanced Materials Division, for XRD experiments. We are thankful to Dr. V. K. Jain, Head, Chemistry Division for his support and encouragement in this activity.

Indigenous technology development: Seismic Switch for Nuclear Reactors

Shiju Varghese, Jay Shah, P.K. Limaye, N.L. Soni and R.J. Patel

Refuelling Technology Division

After Fukushima incident it has become a regulatory requirement to have automatic reactor trip on detection of earthquake beyond OBE level. Seismic Switches that meets the technical specifications required for nuclear reactor use were not available in the market. Hence, on Nuclear Power Corporation of India Ltd (NPCIL's) request, Refuelling Technology Division, BARC has developed Seismic Switches (electronic earthquake detectors) required for this application. Functionality of the system was successfully tested using a Shake Table. Two different designs of seismic switches have been developed. One is a microcontroller based system (digital) and the other is fully analogue electronics (analog) based. These switches are designed to meet the technical requirements of Class IA systems of nuclear reactors. It is also designed to meet other qualification tests such as EMI/EMC, climatic, vibration, and reliability requirements. In addition to nuclear industry seismic switches are having potential use in oil and gas, power plants, buildings and other industrial installations. These technologies are currently available for technology transfer and details are published in BARC website.

This paper describes the requirements, principle of operation, and features and testing of the developed systems.

Introduction

Major earthquakes are known to cause buildings to collapse, dislevel roads, shear pipe lines, disrupt communication, set fires, and inflict injuries which sometimes result in death. While significant advances have been made to reinforce structures against earthquakes, little has been done to reduce non-structural hazards. Topped furniture, objects thrown off shelves and out of cabinets, broken gas and water lines, damaged electric power lines and equipment, derailed passenger trains and elevators, and catastrophic disruption of industrial processes continue to pose a hazard to people and property during a major earthquake. Injuries aside, serious economic losses result from major earthquakes due to the cost of emergency services, repairs, and clean-up.

In this regard, a reliable seismic switch to detect major earthquakes and activate safety devices would be of benefit. One which initiates safety measures before the onset of the earthquakes most destructive ground motions, would be even more so. A forewarning of a few seconds would be most beneficial by warning people to take cover, latching cabinets closed, deactivating electrical equipment, systematically shutting down pipelines, stopping passenger elevators and trains, and putting industrial plants such as nuclear power stations, refineries and electric power plants on standby so as to safely ride out the earthquake, thereby minimizing damage to persons and property.

After Fukushima incident it has become a regulatory requirement to have Automatic Seismic Trip System (ASTS)



Fig. 1: Photograph of Seismic Switch (digital) and its internal PCB's



in nuclear reactors on detection of earthquake. This is designed to scram the reactor upon the occurrence of a seismic event, before turbine trip or other conditions resulting from the seismic disturbance could cause a scram. The earlier scram could give a lead time between 5 to 20 seconds. This lead time could provide resulting benefits such as reduced loads during the seismic event and, therefore, fewer burdens on the plant systems. It may also reduce the likelihood of a Loss of Coolant Accident (LOCA) or severe transient after a seismic event. ASTS comes under classification as safety Class IA system (reactor protection) and has to meet the relevant standard requirements such as on-line testability, fail safe criteria and other qualification requirements. Since systems available in the market are not meeting these requirements, on NPCIL's request, Refuelling Technology Division, BARC has indigenously developed fully functional prototypes of Seismic Switch. Two different designs of seismic switches have been developed. One is a microcontroller based system (digital) and the other is fully analogue electronics (analog) based. Functionality of these systems was successfully tested using a Shake Table. Photograph of the Seismic Switch is shown in Fig. 1.

Theory of Operation

To mitigate the seismic hazard, an NPP is designed to withstand the effects of vibratory ground motion arising from strong earthquakes. The design basis ground motion (DBGM) for this purpose is evaluated for each site. The DBGM is characterized by Peak Ground Acceleration (PGA), response spectral shape and a time history compatible with response spectrum [1]. PGA and response spectrum are derived based on site specific studies. The DBGM parameters are evaluated for two levels of severity, S1 level earthquake or OBE and S2 level earthquake or SSE. The structures, systems and components (SSC) of the nuclear reactors are designed for either SSE (Safe Shut down Earthquake) Level or OBE (Operation Basis Earthquake) level earthquake.

Triggering Conditions of Seismic Switch

The destructive low frequency vibrations (0.05 to 10 Hz) are characteristic of major earthquakes. The seismic switch continuously measures the accelerations in X, Y (Horizontal) and Z (vertical) from the 3-axis MEMS accelerometer. Acceleration signal from each axis is low pass filtered with 3 db cut-off frequency at 13.5 Hz. The Seismic switch triggers on detecting the acceleration greater than the preset PGA level. The PGA level setting is normally kept as the PGA of the OBE level response spectrum of the respective sites. For example; OBE spectra of Tarapur (Maharashtra) site is having a PGA of 0.100g.

Standardised Cumulative Average Velocity (CAV)

Using PGA as the parameter for detection of earthquake often leads to false alarm. Standardised Cumulative Average Velocity can be used as the parameter for detection of earthquake. CAV is the area under the absolute accelerogram as shown in the following equation..

$$CAV_{total} = CAV_i + \int_{t_{i-1}}^{t_i} |a(t)| dt$$

a(t)= acceleration values in a one-second interval where at least one value exceeds 0.025g

i = 1 to n equal to the record length in seconds.

Design Features of Seismic Switches

Seismic Switch is housed in an IP66 industrial rated enclosure with a single cable inlet for all connections. Two outputs are provided in the Seismic Switch which are 2 Form C (DPDT) isolated relay contacts. One is called 'Earthquake relay' and other is called 'Status relay'. Activation or triggering conditions of both the relays are defined.

Coils of both the relays are in energized state during normal operation and de-energizes on any fault. This ensures 'fail safe' operation of the system. On-line testability is another important feature in this system which enables the user to manually initiate the self-diagnostics of the system without removing it from the installation.

Self diagnostics feature of the Seismic Switch (digital) involves continuous health monitoring of communication, battery and sensor parameters. This is carried out in every sensor communication cycle. On any error the earthquake relay gets triggered.

Actual testing of sensor by applying known test condition is carried out during Self Test. It can be initiated manually through push button switch. Self test of Seismic Switch (digital) can be initiated from remote software. It is also done automatically at regular time intervals as well as at reset. Seismic switch generally does not require calibration; however, the calibration can be verified on a tilt table. Seismic Switch (Digital) can communicate to a Graphical User Interface Software (GUI) through an RS-485/RS-232 link. Various features of this software include remote reset for automatic levelling, self test, password protected access, saving instrument details in EEPROM, setting trip parameters, display of battery status, real-time plots of accelerations and display of various other system parameters such as voltage and temperature of the sensor. The system can be programmed for having additional triggering conditions such as Cumulative Average Velocity (CAV).

Testing and Qualification

A Six Degrees of Freedom (6DOF) Shake Table available in Engg. Hall 3 of BARC has been utilized for testing and validating the functionality of Seismic Switches. Sinusoidal motion was created on the table on various peak acceleration amplitudes and actuation of earthquake relay on the preset acceleration amplitude was observed. Response spectrum compatible acceleration time history with Peak Ground Acceleration (PGA) of 0.1g was generated on the table in all three directions individually and simultaneously and actuation of Earthquake Relay was observed. Block diagram of the test setup for all functional and qualification tests are as shown in Figure 2.

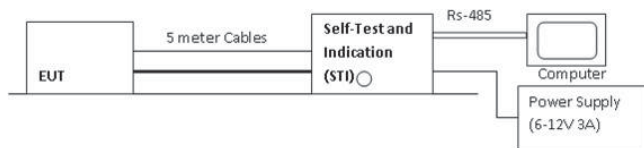


Fig. 2: Test Setup for Seismic Switch.

Seismic Qualification test (Five times Tarapur Spectra with 0.4g PGA on Shake Table) was carried out on the shake table (Figure 3). Visual inspection after the test was carried out and observed that mechanical integrity of the Seismic Switch is intact after the tests.

Seismic switch is designed as a safety critical system for Indian nuclear reactors, which is intended to reliably generate a trip signal to the reactor in the event of an earthquake beyond site specific threshold level. Care has been taken in selection of individual components to have high reliability. Hardware reliability analysis of the Seismic Switch designs have been

analyzed as per MIL HDBK 217 PLUS and found to have MTBF values above 75 Years.

Also, it has to avoid generating spurious trips to meet the relevant standards. This requirement is largely addressed by having 2/3 logic in the nuclear installations. In order to qualify for the nuclear reactor use it has to undergo various qualification tests such as environmental (EMI/EMC and Vibration) and climatic (damp heat, dry heat and temperature cycling) tests. Severity levels of various tests are chosen depending on the operating envelop of the seismic switch installations. Possible Disturbance Sources considered are Lightning, switching inductive loads, arcing, welding, mobile phones, walkie-talkie, voltage sag from starting a large motor, equipment failure, relay actuation (arcing) and cable crosstalk.

CONCLUSION

Seismic Switches are required to trip the Nuclear reactor in case of a Seismic event beyond a threshold level specific to the site. Seismic Switches come under reactor protection system (Class-IA) and it is required to have features such as on-line testability, fail safe and calibration methods. Two different designs (Digital and Analog) were designed, developed and tested on a Shake table.

Seismic Switch (analog) is exempted from Software Verification and Validation (V&V). Components used in the systems was carefully chosen for high reliability and has MTBF of above 75 years as per MIL HDBK 217 PLUS. Functional and Seismic qualification tests were conducted and observed satisfactory performance of these systems. Environmental qualifications tests were selected as per the

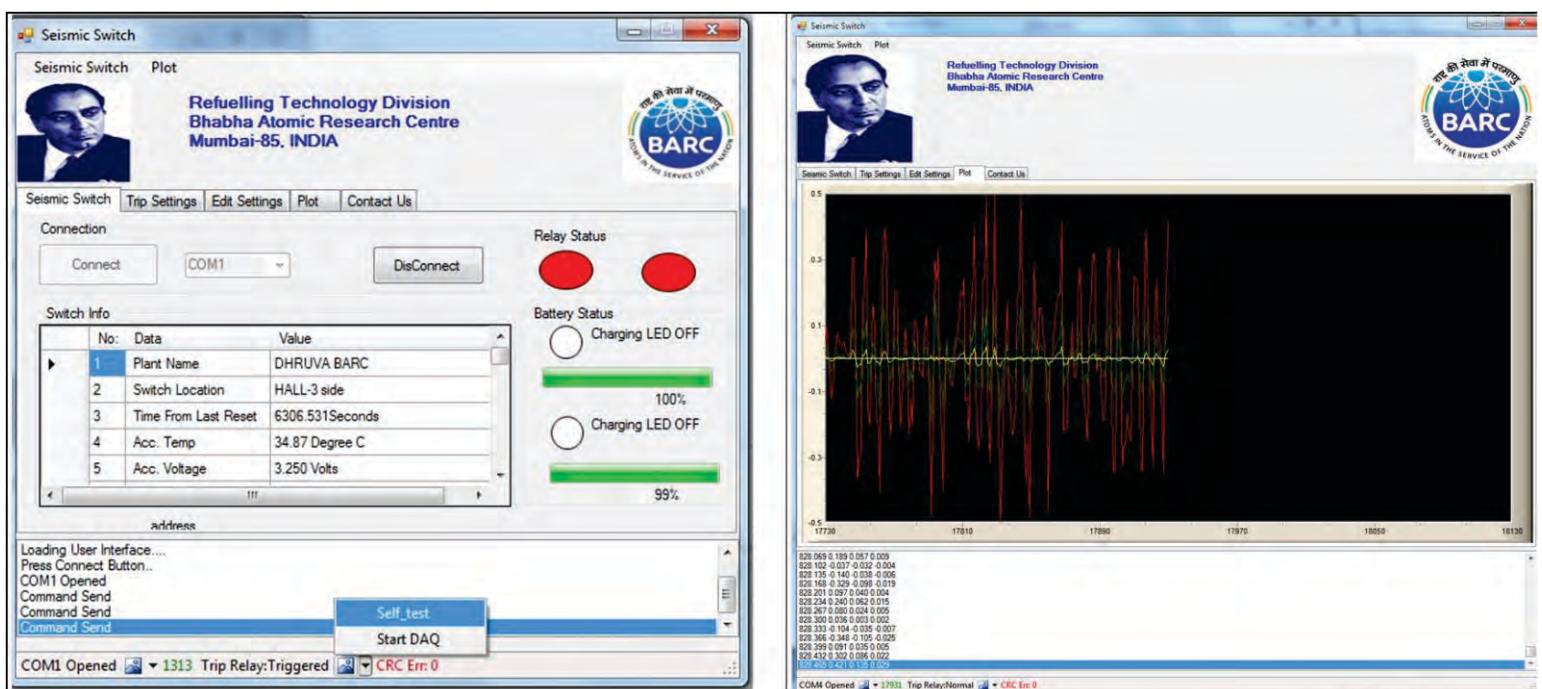


Fig. 3: GUI of the Seismic Switch captured during Seismic qualification testing of the Seismic Switch

operating environment of Seismic Switches. Test setup and procedures have been laid out.

These technologies are currently available for technology transfer and details are published in BARC website.

Acknowledgment

Authors are thankful to Shri. M. Bharatkumar, Associate Director, NPCIL; Shri. M.G Kelkar, Chief Engineer, NPCIL; Shri. V.J Ingle, Additional Chief Engineer (ACE), NPCIL and Shri, Subasish Das, ACE, NPCIL for providing opportunity to develop the Seismic Switches.

Authors sincerely thank Smt. Gopika Vinod, Head, Probabilistic Safety Section and Shri. Santhosh, Scientific Officer (E), Reactor Safety Division, BARC for their support in the hardware and software reliability analysis of the seismic switch.

References

1. Monograph on “Seismic Safety Of Nuclear Power Plants” Ajai S. Pisharady, Roshan A. D, Vijay V. Muthekar; Civil & Structural Engineering Division ,Atomic Energy Regulatory Board (AERB), India
2. Monograph on “Siting Of Nuclear Power Plants” Roshan A.D, Shylamoni P, Sourav Acharya; Civil & Structural Engineering Division, Atomic Energy Regulatory Board (AERB), India
3. AERB Safety Guide: AERB/NPP-PHWR/SG/D-25, Computer Based Systems Of Pressurized Heavy Water Reactors.
4. “Hardware Reliability Analysis Report of Seismic Switches”; Smt. Gopika Vinod, Probabilistic Safety Section, Reactor Safety Division, BARC.
5. Technology Transfer Documentation of Seismic Switches (unpublished).

TAFICS Theme Meeting on I&C SECURITY PROGRAM FOR NUCLEAR FACILITIES

Task Force for Instrumentation & Control (I&C) Security (TAFICS), a DAE level task force organised a Theme Meeting on “I&C Security Program For Nuclear Facilities”, 1-2 April, 2016 at BARC. The meeting was supported by BRNS. I&C security deals with protecting computer-based I&C systems from cyber attacks. The objective of the meeting was to elucidate all stake holders of I&C security – CISOs, ISOs, designers, O&M personnel, senior management - of various DAE units: the purpose, scope and technical details of the I&C security program; the methodology for adapting the security plan and controls for a specific nuclear facility; and expected deliverables of the I&C security program.

The two-day theme meeting was attended by about 125 participants from all over DAE: BARC, NPCIL, IGCAR, AERB, BHAVINI, HWB, NFC, DAE HQ and ECIL.

Shri R.M. Suresh babu, Head EISD, BARC and Convener, TAFICS explained the difference between I&C security and IT security and about the future endeavours of TAFICS. Shri G.P. Srivastava, former Director, E&I Group, BARC described how the physical and computer security issues and solutions have evolved in DAE for the last two to three decades. Shri S.A. Bhardwaj, Chairman, AERB appreciated the work done by TAFICS and said that AERB will develop regulatory documents that deal with I&C security. He also brought out the need to evolve methodology for qualification of commercial off-the shelf (COTS) systems, which are extensively used, particularly in imported reactors. Delivering the Guest of Honour lecture, Dr. Anil Kakodkar emphasised

that I&C security is an important topic and is very dynamic, which requires that the technology used should continuously be updated to keep us ahead of the adversaries. He also advised to develop more in-house products for critical applications and that DAE should make necessary human resources available to TAFICS to carry out the important tasks. The Chief Guest, Dr. R. Chidambaram called up to create a trustworthy cyber eco-system. He also said that there is security in isolation and this should be borne in mind while designing critical computer systems. He advised TAFICS to interact with critical infrastructure security forums to understand the emerging threat vectors and vulnerabilities of computer systems. Dr. R. Chidambaram released the second implementation guide published by TAFICS, titled “I&C Security Program for Nuclear Facilities”.



Panel Discussion : Shri K.K.M. Haneef, Shri Bharath Kumar, Shri R.K. Patil, Shri G.P. Srivastava, Shri B.B. Biswas, Shri R.S. Mundada, Shri R.M. Suresh babu



Release of TAFICS Implementation Guide. Shri S.A. Bhardwaj, Dr Anil Kakodkar, Dr R. Chidambaram, Shri G.P. Srivastava, Shri R.M. Suresh babu

View of audience



Following the inaugural session, there were six sessions, in which nineteen experts in this field delivered talks on all aspects of I&C security. The topics included: I&C security plan, I&C security controls, safety-security interface, security issues during design and implementation, hardware Trojans, COTS systems security issues, cyber DBT, risk assessment and procurement & supply chain issues. One session was dedicated to talks on security-sensitive products that are developed in-house – which can be used by the users

across DAE units - and product endorsement scheme of TAFICS.

The theme meeting had a panel discussion chaired by Shri G.P. Srivastava that brought forth a number of questions from audience related to I&C security implementation. The meeting ended with a note that it was very information and educative and using the guide published by TAFICS, all relevant DAE units should strive towards building a robust defence for I&C security.

Thirty First Training Course on “Basic Radiological Safety and Regulatory Measures for Nuclear Facilities”

BARC Safety Council Secretariat (BSCS) conducts a series of short-term training courses on “Basic Radiological Safety and Regulatory Measures for Nuclear Facilities” for the staff of BARC, to impart general awareness on radiological safety, industrial safety and regulatory requirements. The 31st Training Course was conducted during March 28-31, 2016 for the officers of Nuclear Fuels Group (NFG) and Nuclear Recycle Group (NRG).

The training programme was inaugurated on March 28, 2016 at B-Block Auditorium of Modular Labs. Shri K.Jayarajan, Head, BSCS welcomed the dignitaries and participants to the function. Shri Y.K.Taly, Chairman, BARC Safety Council introduced the syllabus and their relevance. He explained the importance of regulatory measures in controlling radiation exposure and adherence to safety procedures. Chief Guest of the function, Dr. (Smt.) S.B. Roy, Associate Director, Chemical Engineering Group emphasised on the safety aspects and strict adherence to the regulatory codes, guides and recommendations. She advised the participants to extract maximum benefits from the programme and to share the acquired knowledge among their colleagues. She complimented BSCS for their efforts to spread safety awareness in BARC. The inaugural function was graced by Shri K. Banerjee, AD, NRG and Shri R.P.Raju, Controller, BARC. The Course Director, Shri R.P.Hans, BSCS proposed vote of thanks.

The training course was organised by Shri C.L.R.Yadav, BSCS and his team. About fifty participants upto the grade of SO/D attended the course. It was carried out through classroom lectures and demonstrations. Site visits to Emergency Response Centre and Dhruva Reactor were arranged. Faculty members include experts from Health Physics Division, Radiation Safety Systems Division, Radiological Physics &

Advisory Division, Medical Division, Industrial Hygiene & Safety Section and Fire Services Section, in addition to the officers from BARC Safety Council Secretariat. The training programme covered radiation protection programme in back-end and front-end nuclear fuel cycle facilities; dosimetry and dose control; environmental radiation monitoring around nuclear facilities; occupational health care and management of internal contamination; preparedness and response for nuclear and radiological emergencies; biological effects of radiation; safety culture and regulatory framework for BARC. A written test was conducted at the end of the course.



Chief Guest Dr. (Smt.) S.B.Roy, AD, ChEG releasing the compiled lecture notes. Shri Y.K.Taly, Chairman, BSC; Shri K. Banerjee, AD, NRG; Shri R.P.Raju, Controller, BARC and Shri K.Jayarajan, Head, BSCS are also present on the dais.

Certificates were distributed to all participants during valedictory function held on March 31, 2016. The function was graced by Dr. Pradeep Kumar, AD, Health Safety & Environment Group; Shri Y.K.Taly, Chairman, BSC; Shri Vivek Bhasin, AD, NFG; Dr. D. Datta, Head, RP & AD; and Shri K. Jayarajan, Head, BSCS. Feedback on the training programme was taken from the participants for improving the future training programmes. The training programme was well appreciated by all the participants.



Participants of the training programme, along with Shri Y.K.Taly, Chairman, BSC; Shri Vivek Bhasin, AD, NFG; Shri K.Jayarajan, Head, BSCS; Dr. D. Datta, Head, RP&AD; Shri R.P. Hans, BSCS and invitees after the valedictory function.

Technology Transfer to Industries

During the period between December 2015 and March 2016, BARC has transferred fourteen technologies to various industries. Technology Transfer & Collaboration Division (TT&CD) co-ordinated these technology transfers. The details are given below:

A. “Bicycle Mounted Water Purification (Ro/Uf) Unit Driven by Hybrid Power System” Technology was transferred to M/s Oasis Aqua Ventures Pvt. Ltd., Andheri (E), Mumbai, on December 3rd, 2015

This technology is an adaptation of conventional RO & UF. The unit is an off-grid, stand-alone, bicycle mounted brackish water reverse osmosis (BWRO) system of 10 -20 litres/hr (lph) capacity which can treat water contaminated with, salinity (up to 1000 mg/l), toxic elements, pathogens & turbidity. It can be operated throughout the day with the help of the dual energy systems provided. The same unit can be modified by incorporating an Ultrafiltration (UF) membrane, for removing only pathogens & turbidity from the raw water. In such case, the production will be increased to 120-200 lph.



Photograph after signing the agreement with M/s Oasis Aqua Ventures Pvt. Ltd., Mumbai, from left to right, Shri Dipankar Das , Manager, M/s Oasis Aqua Ventures Pvt. Ltd., Shri B.S.V.G. Sharma, Head, TT&CD, Shri Bhaskar Pandey, Executive V.P., M/s Oasis Aqua Ventures Pvt. Ltd., Shri D. Goswami, Head, DD, Smt. S.T. Panikar, Head, PDUS, DD and Shri S. N. Dutta, TT&CD.

B. “Dustline Respirator and Airline Respirator” Technology was transferred to M/s. Venus Safety & Health Pvt. Ltd., Navi Mumbai on December 14th, 2015

BARC has developed Dust respirators and airline respirators as an import substitutes to meet the stringent requirements needed for use in highly toxic environment. Dust respirator is an air-purifying respirator. It is a half-

mask respirator, which covers nose and mouth. Normally the mask is fitted with a pair of high efficiency filters to provide protection in an environment contaminated with fumes, mists, highly toxic particulates including radio nuclides. Respirator can also be fitted with a pair of combination (impregnated charcoal + HEPA) filter cartridges to remove organic and iodine vapours in addition to particulates from breathing atmosphere.

Airline respirator is a continuous flow air-supplied respirator. It has a half-face mask to which respirable air at the rate of 120 l/min is continuously fed by means of an air-hose. Positive pressure inside the face-piece gives very little possibility for outside contaminated atmosphere to leak in. Airline respirators are mainly used in conjunction with plastic suits to provide air for breathing, the latter to prevent skin contamination in all the nuclear facilities.



Photograph taken during the occasion of signing the agreement with M/s. Venus Safety & Health Pvt. Ltd., Navi Mumbai seen from L-R, Shri G. Ganesh, Head, ORPRS, HPD, Shri B S V G Sharma, Head, TT&CD, Shri Mahesh Kudav, Managing Director, M/s. Venus Safety & Health Pvt. Ltd., Shri Ravi Shinde, Manufacturing head, M/s. Venus Safety & Health Pvt. Ltd., Shri G. R. Ursal, SO/F, TT&CD and Shri D. S. Patkulkar, SO/E, HPD.

C. “Compact SMPS Based Triode Sputter Ion Pump Power Supply” Technology was transferred to M/s ECIL, Hyderabad on January 13th, 2016.

This technology of was developed by Technical Physics Division, BARC. This supply can be used with Triode Sputter Ion Pumps having pumping speeds up to 140 lps and for Thin film deposition by DC magnetron sputtering technique. Sputter ion pumps find extensive use in high vacuum systems where a “clean” vacuum is

desired. They are used in scanning probe microscopy and other high-precision apparatuses.

Conventional Sputter ion pump power supplies tend to be heavy and bulky as they operate on the mains frequency viz. 50Hz. The compact switched mode triode sputter ion pump power supply made in BARC is based on a half bridge dc to dc converter operating at 20kHz resulting in a drastic size reduction of around 75% over conventional mains frequency operated ion pump power supplies. Our compact SMPS triode sputter ion pump power supply is rated for an open circuit voltage in the range of -6kV to -7kV with a short circuit current rating of 200mA. This supply can power triode sputter ion pumps of ratings up to 140 liters / second. A microcontroller circuit is used to display the various parameters, implement the Trip logic and provide a PC interface.

D. “Soil Organic Carbon Detection Kit (SOCDK)” Technology was transferred to M/s Precixon, Nashik, (Maharashtra), on January 20th, 2016.

The technology of “Soil Organic Carbon Detection Kit (SOCDK)” has been developed by Nuclear Agriculture and Biotechnology Division, BARC. This kit analyses organic carbon content of soil directly on the field. This kit has been devised to help farmers to understand the carbon status of his field which ultimately decides the yield of crop. It gives quick results and thereby enables farmer to take corrective measures for maintaining soil fertility especially before sowing and at the harvest of any crop. The detection method works on the basis of organic matter extraction from the soil. The extraction is enhanced by addition of chemicals provided in the kit. The colour developed after extraction shall be compared



Photograph after signing the agreement with M/s Precixon, Nashik, seen from left to right, Dr. S. T. Mehetre, NA&BTD, Dr. Yuvraj Vijay Patil, partner and Shri Atish N Pawar, partner, M/s Precixon, Shri B.S.V.G. Sharma, Head, TT&CD, Dr. S.P. Kale, Head, NA&BTD and AD, BSG (A), Shri S. N. Dutta, TT&CD, Shri V. K. Upadhyay, TT&CD.

with chart provided for estimation of organic carbon content of the soil. Estimation of soil organic carbon content becomes easy to perform, giving immediate results and useful to farmers for their own use.

E. “Peripheral Pulse Analyzer” Technology was transferred to M/s Balaji Electronics & Solutions, Mumbai on January 27th, 2016

This Technology has been developed by Electronics Division, BARC. It is a computer based system for the study of physiological variabilities. It has unique feature that it yields heart rate variability, respiration rate variability, cardiac output variability/ peripheral blood flow variability from a single data acquisition session from the patient. The picture shows Peripheral Pulse Analyzer system in operation developed at BARC. The data acquisition is controlled by the PC, serially connected to the acquisition unit. The variability analysis and transfer to database is performed by the PC with the help of Peripheral Pulse Analyzer package in post processing module.



Photograph after signing the agreement with M/s Balaji Electronics & Solutions, Mumbai, seen from left to right, Smt. Anita Behere, ED, Shri. R. K. Jain, ED, Dr. D. Das, Head, ED, Shri. B. S. V. G. Sharma, Head, TT&CD, Shri. Vinit Sinha, ED, Shri. Ragavendra Rao, M/s Balaji, Smt. Sadhana Mandlik, ED and Smt. Smita S. Mule, TT&CD

F. “Handheld 12 Channel Tele ECG Instrument” was transferred to M/s Cardea Biomedical Technologies (P) Ltd., New Delhi on February 1st, 2016

Electronics Division, BARC has developed a Handheld 12-Channel Tele-ECG Instrument operated with the help of a mobile phone via Bluetooth. It records all the 12-leads of ECG simultaneously and displays the same on mobile screen. After complete recording, the report is generated in the form of an image that can be sent to the expert's mobile through Multimedia Messaging Service (MMS) or any other file sharing apps. The device is ideally suited

for rural health care. In city hospitals, the machine can be operated through Laptop/Desktop and report can be shared on Local Area Network (LAN). ECG report in standard graphical format can be taken on a blank A4 size paper.

This has provided virtual instantaneous ECG diagnostic service to a villager at his home/village thus, proving the philosophy – “Cardiac Care – Just a Click Away”.



Photograph after signing the agreement with M/s Cardea Biomedical Technologies (P) Ltd., New Delhi, seen from left to right, Shri. Vinit Sinha, ED, Shri. R. K. Jain, ED, Dr. D. Das, Head, ED, Shri. Abhinav, M/s Cardea, Shri. B. S. V. G. Sharma, Head, TT&CD, Smt. Smita S. Mule, TT&CD and Smt. Soniya Murudkar, TT&CD

G. Automated Alpha Particle Irradiator – Bio Alpha” Technology was Transferred to M/s Anden Mechstronics Pvt. Ltd., Mumbai on February 8th, 2016

H. “Mass multiplication medium of bio-fungicide Trichoderma spp.” and “A purely organic, seed dressing bio-fungicide formulation of an improved Trichoderma Virens Mutant Strain” technologies were transferred to M/s. Ponalab Biogrowth Private Ltd, Bangalore on February 9th, 2016

• “Mass multiplication medium of bio-fungicide Trichoderma spp.” Technology:

Nuclear Agriculture and Biotechnology Division, BARC has developed a low cost mass multiplication medium for faster growth of Trichoderma spp. This material supports better growth of biofungicide compared to existing methods and addition of synthetic sticker is not required while making its formulation. The process is cheaper than the existing methods and is based on the material which is inexpensive and available locally. Hence, in true sense this technology generates wealth from waste.

• “A purely organic, seed dressing bio-fungicide formulation of an improved Trichoderma Virens Mutant Strain.” technology:

Biological control is an integral component of organic farming, but almost all the commercial Trichoderma formulations contain synthetic additives like the carboxy-methyl cellulose (CMC). Nuclear Agriculture and Biotechnology Division, BARC has developed a purely organic, granular, seed treatment formulation of an improved Trichoderma Virens Mutant Strain. A mutant strain of Trichoderma virens produces more antibiotics than the wild type. The purely organic (no chemical additive) granular, seed dressing formulation, named as “TrichoBARC” is suitable for packaging in small quantity (5 g for treatment of 1 kg seeds, per pouch), thus reducing the cost of seed treatment, making it economical for even small and marginal farmers



Photograph after signing the agreement with M/s. Ponalab Biogrowth Private Ltd, Bangalore seen from left to right, Shri Naresh Yavvara, Production Supervisor, M/s. Ponalab Biogrowth Pvt. Ltd., Shri Sharan Basava Sadashivappa, Production in Charge, M/s. Ponalab Biogrowth Pvt. Ltd., Dr. S. T. Mehetre, NA&BTD, Shri BSVG Sharma, Head, TT&CD, Dr. Dinesh Shetty, Managing Director, M/s. Ponalab Biogrowth Private Ltd., Dr. S. P. Kale, Associate Director, Bio Science Group, (A), Dr. P. K. Mukherjee, NA&BTD and Shri G. R.

I. 3kJ/s, 30kV Capacitor charging Power Supply’ Technology was transferred to M/s Artech Welders, Pune on February 16, 2016

This technology was developed by Accelerator and Pulse Power Division, BARC. Capacitor charging supplies differ from conventional DC supplies in that the output current is fixed and not variable, allowing the load capacitor to be charged in the fastest possible time, with no requirement for series current limiting resistors. Capacitor charging power supplies are specifically

designed to efficiently charge capacitive loads to high voltages with excellent pulse to pulse repeatability at very high repetition rates. The largest application for this type of supply is in the laser industry. In addition it also has applications in areas as diverse as medical sterilization and rock crushing. Capacitor charging power supply is used in various accelerators, pulse forming line, RF systems, capacitor banks, magnet supply etc. It can act as a power source of arc lamps, flash lamps, and flash x-ray systems. It can be used as a charging source for various kinds of repetitive laser system like excimer lasers, free electron lasers. It has various uses in repetitive pulse power systems like electromagnetic forming, repetitive Marx based pulse power systems, magnetic switch based repetitive pulse power system. It has inherent safety features from over current and short circuit protection. Irrespective load it supplies constant current to the load at prescribed charging rate.



Photograph after signing the agreement with M/s Artech Welders, Pune seen from left to right Shri A.S. Patel, APPD, Dr. Amar Banerji, TT&CD, Shri Subhash V. Patwardhan, Director, M/s Artech Welders, Shri B.S.V.G. Sharma, Head, TT&CD and Dr. Archana Sharma, APPD

J. “Triode Sputter Ion Pump” Technology was transferred to M/s Tulasi Engineering Works, Patancheru, Telangana, on February 18, 2016.

This technology was developed by Technical Physics Division, BARC. Sputter Ion Pumps are to produce very low pressures (typically 10^{-9} mbar) in closed and clean vacuum systems without any hydrocarbon contamination. These pumps are mainly used in applications involving transportation of charged particle beams (electrons, ions) in particle accelerators, storage rings for generation of synchrotron radiation, analytical equipment such as mass spectrometers, x-ray photoelectron spectrometers, etc. as well as in Semiconductor industry. It provides clean and completely oil-

free ultrahigh vacuum. The pumps can be connected in any orientation and require very low power to operate under stable static conditions. This ensures that the pumps has very long working life (typically > 50,000 hours), virtually maintenance free and are easy to install and operate unattended for long periods of time. Inherent protections in the power supply enable the prevention of arcing and high discharge current at high pressures. Sputter ion Pumps with pumping speeds 35 lps, 70 lps, 140 lps and 270 lps have been developed and are included in the technology transfer.



Photograph after signing the agreement with M/s Tulsi Engineering Works, Telangana seen from left to right Dr. Amar Banerji, TT&CD, Dr. K. G. Bhushan, TPD, Shri R. V. Satyanarayana Reddy, M/s Tulasi Engg. Works, Shri R. V. Krishna Reddy, Proprietor, M/s Tulasi Engineering Works, Shri B. S. V. G. Sharma, Head, TT&CD, Dr. S. K. Gupta, Head, TPD, Shri Kavindra Pathak, TPD, Shri Prakash Abichandani, TPD and Shri V. Perayya, TPD

K. “Partially Hydrolyzed Guar Gum for Dietary Fibre Application” Technology was transferred to M/s Adachi Natural Polymer Pvt. Ltd., Ahmedabad on March 14th, 2016

L. Nisargruna Biogas Technology based on biodegradable waste has been developed by NA&BTD. The plant processes biodegradable waste into biogas and weed free manure. It was transferred to the following parties:-

- M/s Excellent Renewables Pvt. Ltd., Gujarat on 30.12.2015
- M/s Western Biosystems (I) Pvt. Ltd., Hyderabad on 12.01.2016

M. BARC through its Centre for Incubation of Technology has signed the MoU with with M/s Larsen & Toubro Limited (L&T), Bangalore For Incubation Of “Development Of Residual Gas Analyzer (RGA)” on February 8th, 2016

Residual Gas Analyzer (RGA) is a compact, usually flange mounted mass spectrometer, typically designed for process control and contamination monitoring in

vacuum systems. Based on an electron impact ion source and a quadrupole mass analyzer, RGAs are used in high vacuum applications such as research chambers, surface science setups, accelerators, scanning microscopes, etc.

RGAs are used in most cases to monitor the quality of the vacuum and detect trace impurities in the low-pressure gas environment. RGAs possess sub-ppm detection capability in the absence of background interferences and impurities can be measured down to 10-14 Torr levels. RGAs can also be used as sensitive in-situ, helium leak detectors. With vacuum systems pumped down to lower than 10⁻⁵ Torr - checking of the integrity of the vacuum seals and the quality of the vacuum - air leaks, virtual leaks and other contaminants at low levels may be detected before a process is initiated.

M/s Larsen & Toubro Limited is interested in jointly developing the RGA technology for industrial use. A possible offshoot of this technology is the coupling of RGA to a Gas Chromatograph Mass Spectrometer (GCMS) system being developed for Defence Research & Development Establishment (DRDE) to detect warfare/explosive agents.

As per this incubation MoU, R&D efforts will be undertaken at Technical Physics Division, (TPD), to

develop suitable technology. Initial experiments carried out at Technical Physics Division, have been encouraging and further work is in progress with active participation of the incubatee (M/s Larsen & Toubro Limited).



Photograph after signing the agreement with M/s Larsen & Toubro Limited (L&T), Bangalore. Seen from left to right, Shri A.M. Kasbekar, TPD; Shri V. Nataraju, Head, AMSS, TPD; Shri Prakash Abichandani, Head, AE&IS, TPD; Shri Raghavendra Rao J, Asst. GM, L&T; Dr. S.K. Gupta, AD, Physics Group and Head, TPD; Shri B.S.V.G. Sharma, Head, TT&CD; Dr. R. Rajagopal, Head, Technology Development, L&T; Shri S. N. Dutta, TT&CD and Shri V. K. Upadhyay, TT&CD.

60th DAE Solid State Physics Symposium-2015 (Diamond Jubilee Year)

The 60th DAE Solid State Physics Symposium-2015 was held at Amity University UP, Noida, Uttar Pradesh during December 21-25, 2015. The symposium was fully sponsored by the *Board of Research in Nuclear Sciences (BRNS)*, Department of Atomic Energy (DAE). Over several decades the symposium has been organized successfully with the symposium entered into its 60th, the diamond jubilee year in 2015. In this Diamond Jubilee Year, Dr. N.K. Sahoo was the convener and the roles of secretaries were discharged by Dr. (Mrs.) R. Chitra and Dr. Shovit Bhattacharyya. This year 763 contributory papers were selected out of 1307 papers that were extensively reviewed by expert scientists from all over the country. Besides, there were 41 thesis and 10 young achiever award presentations and three awards were given in each category.

The symposium was inaugurated by Dr. S.M. Sharma, the then Director, Physics Group, BARC. The keynote address was delivered by Dr. S.K. Sikka. The Scientific sessions were held in time and the plenary talk and invited talks covered diverse topics which are of importance to concurrent scientific, technological, bio-medical, energy, nuclear and advanced material research. There was a plenary talk on first day with titled, "*Condensed Matter Phenomena under High Pressure: Some Insights*" by Dr. S.M. Sharma. There were two evening talks on first as well as second day of this memorable event, titled (i) "*Importance of Materials in a Knowledge Economy*" by Dr. R. Chidambaram and (ii) "*Material Science: a Mythological Perspective*" by Dr. Devdutt Pattanaik respectively, to add extra dimensions to the scientific deliberations.

The topics covered in this symposium through 49 invited talks, 24 oral presentations and over 800 poster presentations

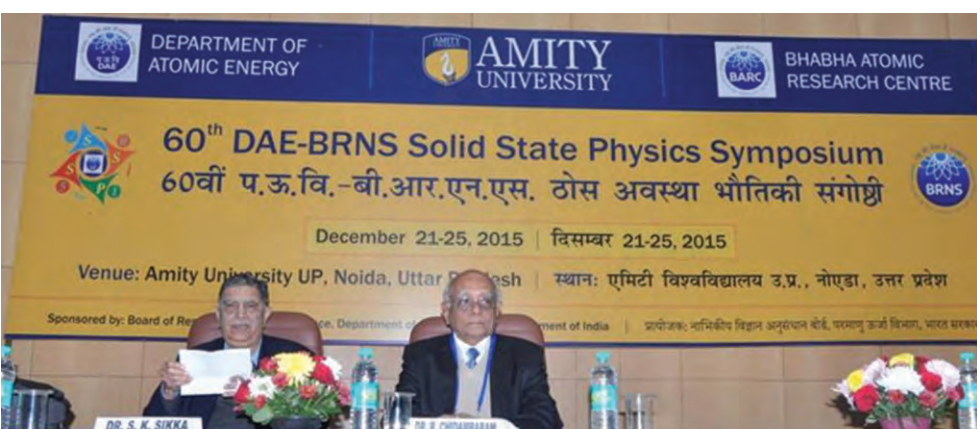
were (a) Phase Transitions, (b) Soft Condensed Matter including biological systems, (c) Nano-materials, (d) Experimental Techniques & Devices, (e) Glasses & Amorphous Systems, (f) Surfaces, Interfaces & Thin Films, (g) Electronic Structure & Phonons, (h) Single Crystals, (i) Transport Properties, (j) Semiconductor Physics, (k) Superconductivity, Magnetism and Spintronics and (l) Novel Materials. The 11 thematic seminars of potential interests to solid state and condensed matter scientific communities included were in the areas of (i) Applied materials, (ii) Thin Films/polymers, (iii) Ion beam Processing/ Accelerator Based Solid State Physics, (iv) Topological Insulator & Nano-Magnetics, (v) Carbon Based materials, (vi) Nano & novel materials, Photonics & Meta materials and Physics Under



Inaugural address by Dr. S.M. Sharma, Director, Physics Group, BARC

extremes and Theoretical Solid State. Apart from these there were two panel discussions I) Neutron Science Researches and II) Synchrotron Science Researches. The symposium as a whole provided a very interactive scientific platform for interaction, discussion and reviewing of the scientific works by students, young and senior research scientists.

The valedictory session was chaired by Dr. S.K. Gupta, the then Associate Director, Physics group who in his concluding address summarized the five-day events. In this symposium 26 awards were given which included 20 best poster presentation awards, 3 Young Achiever's Awards, 3 Best Thesis Awards. On this occasion, a special souvenir was brought out in collaboration with the Indian Physics Association (IPA). Overall this Diamond Jubilee event was memorable on several scientific as well as organizational fronts.



Dr. S.K. Sikka and Dr. R. Chidambaram during the special evening talk session

National Technology Day 2016



Chief Guest Prof. Chaitanyamoy Ganguly, PDPU, Gandhinagar

National Technology Day 2016 was celebrated on 11th May 2016 at Central Complex Auditorium of Bhabha Atomic Research Centre (BARC), Trombay. The Programme started with Invocation song by BARC Cultural Choir. This was followed by Welcome address from Shri. K.N. Vyas, Director, BARC, who highlighted the importance of the day. Peaceful

Nuclear Experiment carried out at Pokhran on 11th May, 1998 was an important milestone achieved by the country and as well as BARC. He further mentioned the coincidence of this year's theme i.e. 'The World of Materials' with the 75 years celebration of Plutonium Discovery. The Presidential address was given by Dr. Sekhar Basu, Secretary, Department of



Inauguration of "World of Materials" exhibition by the chief guest



Shri K.N. Vyas, Prof. Chaitanyamoy Ganguly and Dr. G.K. Dey during exhibition

Atomic Energy (DAE) and Chairman, Atomic Energy Commission (AEC). He emphasized the creditable roles played by materials and material scientists in the field of nuclear science and engineering and in every stages of the nuclear fuel cycle. This year, the Chief Guest for the function was Prof. Chaitanyamoy Ganguly of Pandit Deendayal Petroleum University (PDP), Gandhinagar who is associated with Nuclear Science and Technology for nearly

five decades. His talk on “Plutonium for Peace and Prosperity through Fast Breeder Reactor Technology” was highly appreciated by the audience. Dr. Ganguly was felicitated by Dr. Sekhar Basu. Dr. G.K. Dey, Director, Materials Group offered the 'vote of thanks'. An exhibition on “World of Materials” was organised as a part of the event to showcase the achievements of scientist and engineers of DAE in the area of material science.

BARC Training School Graduation of the 59th batch of OCES and 12th batch of OCDF trainees



The Graduation Function of the 59th Batch of OCES and 12th Batch of OCDF was held in a glittering ceremony in Central Complex Auditorium on July 25th, 2016. Vice Admiral Dinesh Prabhakar, Director General, ATV Programme, DRDO was the Chief Guest for the event.

The event was well organised and began with an invocation by the BARC Choir Group. Introductory remarks by Dr. M.Ramanamurthi, Head, OCES Programme Implementation acknowledged the contributions of a vast number of personnel and agencies involved in the conduct of the Training School Programme. It was heartening sight that the parents of the graduating trainees had also turned up in large numbers to celebrate in the joy and success of their children. In his welcome address, Shri K.N.Vyas, Director, BARC highlighted the importance of the training school as a vehicle for knowledge generation and retention in the arena of nuclear science and technology in the country. He also brought out the importance of continuing R&D to accelerate the programs of the Department and the role of the Homi Bhabha National Institute in catalysing this synergy. He also mentioned the need to monetise the technologies developed as a method of maximising the economic benefits of these developments to the nation.

Shri Sekhar Basu, Chairman, AEC, in his presidential address, mentioned that the Department has 30 institutions



Vice Admiral Dinesh Prabhakar addressing the Training School graduates



Shri K.N. Vyas, Director BARC handing over memento to Vice Admiral Dinesh Prabhakar, Director General, ATV Programme, DRDO

falling under it and mandates in the commercial, R&D and services sectors are to be fulfilled by these institutions. He urged the trainees to be dynamic and positive in their approach to provide out of the box solutions towards ensuring economical and societal benefits to the country. The support from the government has been forthcoming and generous and we need to utilise the opportunity 'to think, to do and to deliver', he said.

The Chief Guest, Vice Admiral Dinesh Prabhakar gave an inspirational talk, focusing on the importance of collaboration and team work which is essential for the success of a project. He also imparted some important life and career lessons to the young trainees, which should stand them in good stead for during the course of their careers. Success he

said, can be achieved by sustained effort over the course of one's life and career. It's important to dream big and work hard towards making it a reality. Dr. A.P.Tiwari in his concluding remarks highlighted the sterling qualities and contributions of the icons of the Department such as Dr. R.Chidambaram, Dr. A. Kakodkar, Dr. S.Banerjee, Dr. R.K.Sinha, Dr. Sekhar Basu and Shri K.N. Vyas and urged the trainees to draw inspiration from them. He went on to thank all agencies, scientists and personnel involved in the conduct of the Training School programme for their support and cooperation.

The national anthem was rendered at the end to bring the event to a resounding conclusion.

Scientists Honoured

- Dr. S. M. Yusuf, SSPD received the 'MRSI-ICSC Superconductivity & Materials Science Annual Prize' for the year 2016 from the Materials Research Society of India (MRSI)



- Dr. Ranjan Mittal, SSPD received Materials Research Society of India (MRSI) medal (2016) for his outstanding contributions in the field of condensed matter research.





Common Name: Prayer Plant, Rabbit's Foot, Herringbone Maranta
Botanical Name: Maranta leuconeura var. erythronera G.S.Bunting
Family: Marantaceae
Location: Nursery of L&CMS